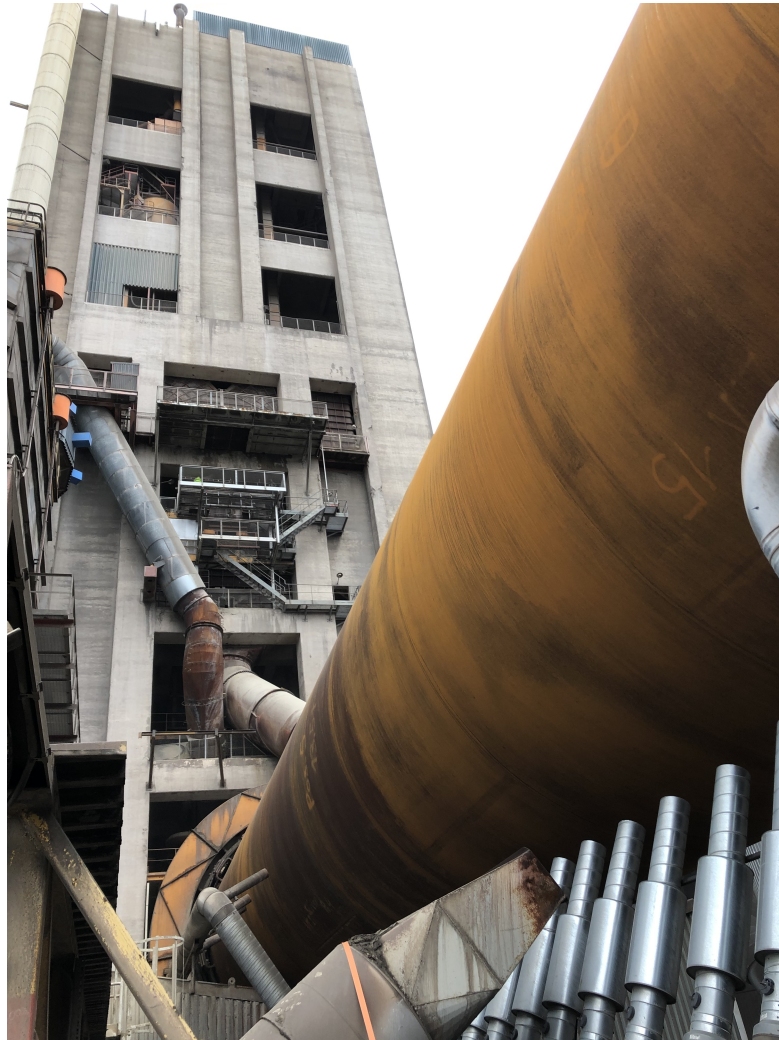




CHALMERS
UNIVERSITY OF TECHNOLOGY



Evaluation of usage of plasma torches in cement production

A heat transfer modelling study

Master's thesis in Master Programme Sustainable Energy Systems

TOVE BURMAN
JOHANNA ENGVALL

MASTER'S THESIS 2019

Evaluation of usage of plasma torches in cement production

A heat transfer modelling study

TOVE BURMAN
JOHANNA ENGVALL



CHALMERS
UNIVERSITY OF TECHNOLOGY

Department of Space, Earth and Environment
Division of Energy Technology
CHALMERS UNIVERSITY OF TECHNOLOGY
Gothenburg, Sweden 2019

Evaluation of usage of plasma torches in cement production
A heat transfer modelling study
TOVE BURMAN
JOHANNA ENGVALL

© TOVE BURMAN, JOHANNA ENGVALL, 2019.

Supervisor: Fredrik Normann and Adrian Gunnarsson, Space, Earth and Environment
Examiner: Fredrik Normann, Space, Earth and Environment

Master's Thesis 2019
Department of Space, Earth and Environment
Division of Energy Technology
Chalmers University of Technology
SE-412 96 Gothenburg
Telephone +46 31 772 1000

Cover: Picture of cyclone tower and rotary kiln of system 8 at Cementa, Slite.

Typeset in L^AT_EX
Printed by Chalmers Reproservice
Gothenburg, Sweden 2019

An Initial Evaluation of Usage of Plasma Torches in Cement Production
A Heat Transfer Modelling Study
TOVE BURMAN
JOHANNA ENGVALL
Department of Space, Earth and Environment
Chalmers University of Technology

Abstract

This work developed and evaluated a heat transfer model for the cement production process, focusing on the rotary kiln but also including the cyclone tower. The purpose of the model is to evaluate the implementation of new heat sources, in this case plasma torches. The rotary kiln model is discretised in angular, axial and radial directions and describes the heat transfer characteristics of the gas, walls, and material in the kiln. The heat transfer includes a description of the radiation, convection, and conduction between the cells. The model also includes the flow of gas and material as well as the mixing within the bed due to the rotation of the kiln. The heat transfer in the cyclone tower is assumed efficient and the units are described by simple heat and mass balances.

The model is validated against two distinctive cases of operational conditions of production line 8 at Cements in Slite. An important part of the work was to define and collect data for the model validation. The model shows good agreement with the measured wall temperatures, considering the outside cooling is not included in the model. The results, such as product temperature and heat absorbed by the bed, are consistent with gathered data using a reasonable gas temperature profile and found equilibrium data.

The requirements of the material to reach the desired quality is key to the process and emphasis is put on how to incorporate these requirements into the heat transfer model. The work concluded that a detailed description of the reaction kinetics and heat of reaction is difficult to include in the model due to its complexity and the maturity of the field. Instead this work recommends that seven heating zones are defined through the kiln where the required residence time and heat is determined externally by experiments or detailed modelling of the cement chemistry. In this way the heat transfer model and bed model could in concert and in an iterative manner decide the required temperature profiles and conditions (e.g. gas concentrations or particle loads) of the gas as well as the dimensions of the kiln to achieve the desired product temperature.

The model was applied to evaluate the implementation of a plasma torch in the cement kiln. Compared to today's combustion of coal and other fuels, the plasma torch will decrease the particle load and change the gas composition. The result shows that significantly ($\sim 400^\circ\text{C}$) higher gas temperatures are required in the kiln with plasma torch operation, to reach the desired bed temperatures. Furthermore, the example highlights the importance of being able to predict the development of the gas temperature profile through the kiln. Here the work recommend future work with measuring or detailed modelling (CFD) of the gas phase temperature.

Keywords: Cement production, plasma torch, process modelling, heat transfer, rotary kiln, equilibrium, CO_2 emissions, CCS.

Acknowledgements

A great thank you to all the people making this thesis possible; friends and colleagues at the division of Energy Technology at Chalmers University of Technology, Cementa and Cementa Research. A special thank you to Bodil Wilhelmsson, Johan Larsson and Stefan Sandelin at Cementa, and to our examiner and supervisor Fredrik Normann and our supervisor Adrian Gunnarsson at Chalmers University of Technology. We are very grateful for the opportunity of getting to be a part of an industry moving towards a greener future.

Last but not least we thank friends, family and especially Emil, Erik, Ludwig, Linus, and David.

Tove Burman and Johanna Engvall, Gothenburg, June 2019

Contents

List of Figures	xi
List of Tables	xiii
Abbreviations & Nomenclature	xv
1 Introduction	1
1.1 Background	1
1.2 Aim	2
2 Theory	3
2.1 The Cement Production Process	3
2.1.1 Process at site in Slite	5
2.2 Plasma Torches	10
2.3 Carbon Capture and Storage	12
2.4 Implementation of Plasma Torches and Carbon Capture and Storage in Cement Production	13
3 Method	15
3.1 Project Method	15
3.2 Equilibrium Data	16
3.2.1 Thermophysical Data	17
3.3 Reference case	17
3.3.1 Cementa Data	17
3.3.2 Overall Energy Balance	18
3.4 The Bed Model	19
3.4.1 Cyclones	19
3.4.2 Calciner	20
3.5 Heat Flux Model	22
3.5.1 Plasma Modelling	24
4 Results and Discussion	27
4.1 Equilibrium Data	27
4.2 Energy Balances	28
4.3 Bed Modelling	31
4.4 Heat Flux Model	32
4.5 Plasma Modelling	37
5 Conclusion	41

6 Suggestions for Further Research	43
Bibliography	45

List of Figures

2.1	A schematic overview of the cement production process	3
2.2	Flow sheet of cyclone tower and calciners of system 8 at Cementa, Slite . .	6
2.3	Pictures of calciner showing inlet of gas, raw meal and flame	6
2.4	Schematic picture of the rotary kiln	7
2.5	Picture of cooling air flow nozzle on the outside of the kiln	8
2.6	Picture of how parts of the brick lining is pulled off	8
2.7	Flow sheet of cooler, showing the different flows of air, clinker and gypsum.	8
2.8	Picture of roster rows in cooler	9
2.9	Picture of nozzle spraying in gypsum in cooler	9
2.10	Picture of crushers in primary cooler	9
2.11	Scheme of linear single-chamber plasma torch with self-setting arc length .	10
2.12	CCS in combination with a cement production process	13
3.1	An overview of the method for this thesis	15
3.2	Temperatures and mass flows used in modelling of cyclones	20
3.3	Mixing point after calciners	21
3.4	Cross-section of a rotary kiln showing different possible heat exchanges occurring, as well as movement, mixing and rotation	22
3.5	Illustration of zones created in the rotary kiln of the heat flux model	23
4.1	How the composition in a mass of 1 g changes through the temperature interval	28
4.2	Mass fractions of the total mass of all species, depending on temperature .	28
4.3	Graph of how the heat of formation varies along the temperature interval in the rotary kiln	30
4.4	Graph of sensitivity analysis results normalised for heat received by bed . .	32
4.5	Graph of the gas temperature profile along the rotary kiln for case 1	33
4.6	Graph of the gas temperature profile along the rotary kiln for case 2	33
4.7	Graph of heat fluxes along the rotary kiln for case 1	34
4.8	Graph of heat fluxes along the rotary kiln for case 2	35
4.9	Graph of how the wall and bed temperatures and reaction heat vary along the rotary kiln for case 1	35
4.10	Graph of how the wall and bed temperatures and reaction heat vary along the rotary kiln for case 2	36
4.11	Graph of the gas temperature profile along the rotary kiln for plasma torch implementation	38
4.12	Graph showing the difference between the axial gas temperature profiles for the plasma modelling and for the coal modelling	38

4.13	Graph of heat fluxes along the rotary kiln for plasma torch implementation	39
4.14	Graph of how the wall and bed temperatures and reaction heat vary along the rotary kiln for plasma torch implementation	39

List of Tables

2.1	Raw meal composition at Cementa, Slite, January-April 2004	5
2.2	Composition of materials in raw meal, after calcination. LOI is the amount of mass lost due to calcination.	7
2.3	Plasma torch data provided by ScanArc	11
3.1	Parameters for heat flux model	23
3.2	Parameters for kiln wall in heat flux model	24
3.3	Specifications of plasma torches modelled	25
4.1	Inlet compositions used in FactSage TM	27
4.2	Total energy need for heating the meal and for all reactions	29
4.3	Energy need for heating the meal and for all reactions in the cyclone tower and rotary kiln	29
4.4	Reaction heat zones for the two operational cases in kiln in MW	30
4.5	Calculated temperatures in the cyclone tower, case 1 and 2	31
4.6	Results from case 1 and 2 with coal burner	36
4.7	Results from plasma modelling	37

Abbreviations & Nomenclature

Abbreviations

C2F	$2\text{CaO} \cdot \text{Fe}_2\text{O}_3$
C2S	$2\text{CaO} \cdot \text{SiO}_2$ - Belite
C3A	$3\text{CaO} \cdot \text{Al}_2\text{O}_3$
C3S	$3\text{CaO} \cdot \text{SiO}_2$ - Alite
CaO	Free lime
CCS	Carbon Capture and Storage
CS	$\text{CaO} \cdot \text{SiO}_2$
DC	Direct Current
Fluff	Waste pressed into pellet
IP21	Cementa's operating data system - Aspen Process Explorer
NO_x	Nitrogen oxides
SLAGA	Melted phase in kiln
Slag	By-product from metallurgical industry
SO_x	Sulphur oxides

Nomenclature

ρ	Density	kg/m^3
A_{cs}	Cross-sectional area	m^2
c_p	Specific heat capacity	kJ/mole K or kJ/kg K
G_g	Gas mass flux	$\text{kg/m}^2\text{hr}$
H	Heat content	W
h_{cv}	Convective heat transfer coefficient	$\text{W/m}^2\text{K}$
h_f	Heat of formation	kJ/mole
M	Molar mass	g/mol
\dot{m}	Mass flow rate	kg/s
T	Temperature	$^\circ\text{C}$ or K
\dot{V}	Volumetric flow	m^3/s
Q	Heat content change	W
q''	Heat flux	W/m^2

Index

b	bed
$conv$	convection
g	gas
N	north
$react$	reaction
S	south

1

Introduction

This thesis was made in collaboration with the cement production company Cementa, the largest producer of building materials in Sweden. Cementa has a vision to have zero emissions of CO₂ during the life cycle of their products by year 2030. To achieve this, the production cost of cement is estimated to be twice as high as of today, according to cost analyses performed by Cementa, but with a better competitiveness of the product due to radical emission reductions [1]. Cementa are continuously working with improving their energy efficiency, to reach zero emissions energy efficiency measures are not enough. To reach this target a project called CemZero has been initiated to investigate technologies for reducing CO₂ emissions. This thesis is part of CemZero and investigates the possibility of implementing plasma burners in the cement production process, which is one of the low-carbon technologies of interest. The report covers theory on cement production and compares the current production process with production process based on electricity which would decrease the CO₂ emissions. [1] The focus of this thesis is to create a model which describes the heat transfer in the current production process, which could then be modified to investigate the process modifications.

1.1 Background

The global warming caused by emissions of CO₂ can be traced to urbanisation and human activity. Worldwide cement production emits around 2.8 billion tonnes of CO₂ annually, equivalent to 8% of the global total, which is a greater amount than any given country apart from China or the US. [2] The floor area of the world's buildings is projected to double in the next 40 years, meaning that the cement production is set to increase by approximately 5 billion tonnes by 2030, an expected yearly production rate increase of 25% compared to today's level [3]. It is therefore important to reduce the emissions from this industry.

Considering the emissions from the process, approximately 35-40% of the total CO₂ emissions in the cement industry is associated with combustion of fossil fuels in order to heat the raw material to temperatures high enough for the calcination and clinker processes [4]. The remaining 60-65% of the CO₂ emissions is due to the calcination reaction itself [5] and cannot be decreased but the emissions could be managed by Carbon Capture and Storage (CCS) or other methods [1]. The focus of this thesis is to investigate how the heating method could be changed from combustion in order to reduce emissions, and to

prepare for future implementation of Carbon Capture and Storage (CCS).

According to Cementa's preliminary investigations report, electrification of the system is a better economical alternative with less energy consumption to reduce their CO₂ emissions than other CO₂ extraction methods, e.g. amine extraction. Implementing electrification would mean no combustion of fossil fuels in the process, leading to a decreased amount of CO₂ out of the stack. In their investigation, existing possibilities, effect on the electrical system and business prerequisites were examined. The heating technologies they have considered are plasma, electrical flow heaters, microwave heating, resistive electrical heating, inductive heating, direct separation reactors and hydrogen combustion. Based on the results of the investigation the preferred alternative for heating in the kiln is plasma torches, with CO₂ as the preferred working gas. For the calcination, a pilot plant with a direct separation reactor is to be put live in April of 2019 in what is called the Leilac project. Another alternative for heating during the calcination is resistive electrical heating. [1]

Sweden is one of few countries with an almost fossil free power system with what can be considered high reliability [6]. The current yearly energy production on Gotland, the island on where the investigated cement plant is situated, is about half of the current need. This is produced by 180 MW wind power and 3 MW solar power installed on the island. To be able to electrify the cement process on the island, an additional 600 MW needs to be installed, as well as additional transmission capacity of 400 MW from the mainland and reinforcements on the internal grid to increase voltage levels to the double and to ensure the security of the grid. [1]

If electrifying a process, such as the cement industry with plasma burners, the limitations associated to it has to be considered. By implementing plasma torches the gas flow through the process can decrease while temperatures in the flame are significantly higher. These factors together with the fact that plasmas are not widely used today, in large scale industry, means that the knowledge about the behaviour and effects that this transition would have on the heat transfer is limited. Therefore it is important to model such a process before implementation to get a rough idea of what happens to the process and what parts might need to be altered.

1.2 Aim

The aim of this thesis is to create a model that predicts the influence on the heat transfer through out the cement process depending on the heat source. The model is applied to evaluate the implementation plasma torches as replacement for oil and coal burners in the rotary kiln. The intended outcomes of the project is; a functional model of the heat transfer in a cement production process, a conclusion on its validity and initial results of replacing conventional burners with plasma torches.

2

Theory

This chapter contains theory on subjects relevant to the thesis, starting with a general description of the process of producing cement clinker. Next, a detailed description of the studied plant is presented. Basic theory on plasma torches and Carbon Capture and Storage is presented, as well as some insight into usage of these in combination with a cement production plant.

2.1 The Cement Production Process

The process of cement production is treating limestone, clay and sand with heat to produce clinker, consisting of calcium silicates and metals, which is ground and mixed with additives to create cement. The different process steps of the cement production are; preparation of raw materials, preheating of raw meal, calcination, clinker reaction, clinker cooling and clinker grinding and storage. These are illustrated in Figure 2.1. [5]

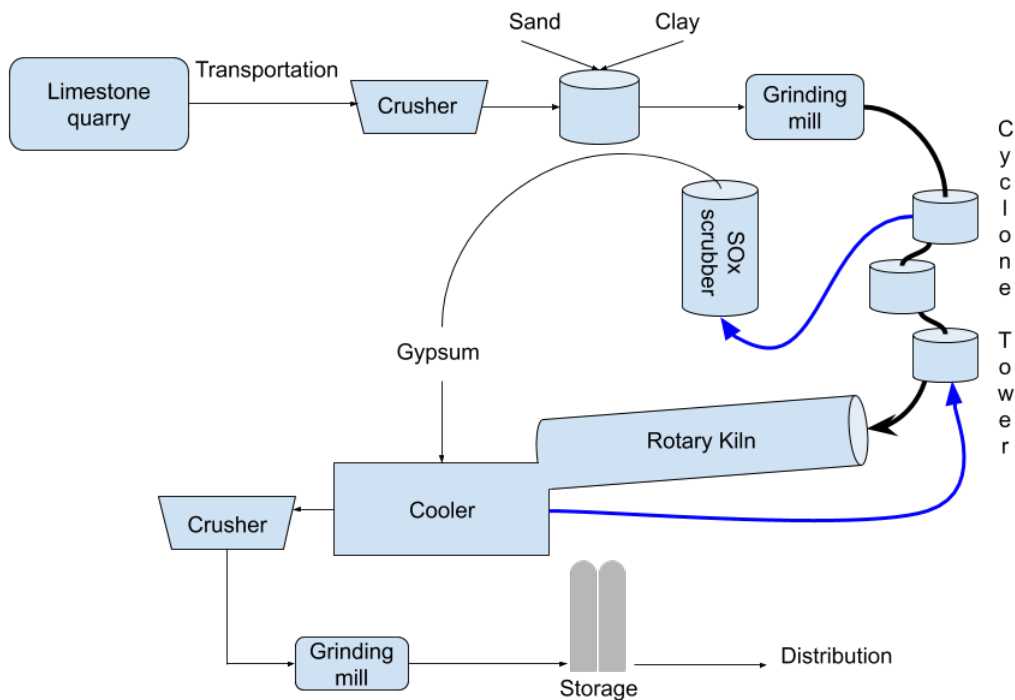


Figure 2.1: A schematic overview of the cement production process

The preparation of the raw material includes crushing of limestone rocks into finer ground limestone, approximately 15-80 mm grains, and mixing with other raw materials such as sand and clay to the desired proportions, see Table 2.1 for an example [7]. After mixing, the raw material is sent to a grinding mill where it is ground further to raw meal, grains of approximately 5-125 μm , and is then dried. Thereafter the raw meal enters the cyclone tower consisting of a series of cyclones where it is heated by swirling hot flue gases from the kiln. After the cyclones the meal enters a calciner, which is part of the cyclone tower, where it is heated through combustion of various fuels. The meal is then separated from the gas in a final cyclone and is fed into the kiln at approximately 900°C. At about 700°C, which is reached in the cyclone tower and calciner, calcium carbonate goes through decomposition into calcium oxide and carbon dioxide, see Reaction 2.1. This reaction is endothermic and continues until all calcium carbonate has been decomposed. [5] However only 95% of the decomposition occurs before the rotary kiln, to prevent clinkerisation in the cyclone tower. [1]



Flue gases exiting the cyclone tower passes through an electro-filter or fabric bag to separate the dust from the gases. Gases are then washed with mild limestone and water in a scrubber to remove SO_x , which forms gypsum that is used as an additive later on in the process. [1] The hot meal enters the rotary kiln where reactions consuming calcium oxide, called clinkerisation reactions, occur. Desired products from these reactions are C3S and other calcium silicates.

The rotary kiln is usually 40-100 m long and has an inner diameter of 3-6 m. The outer shell is made of steel and has an inner refractory lining for thermal insulation. The kiln is inclined 1-3° and rotates with 1-5 rpm to ensure good mixing and a forward motion of the meal. At the kiln outflow a fuel burner is placed to provide heat to the meal to initiate the chemical processes. Primary air enters with the fuel while secondary air enters from the cooler following the kiln. [5]

After the kiln, the produced cement clinker is cooled rapidly to ensure stability of the calcium silicate minerals formed. If the cooling is too slow, alite (C3S), the desired product, can partially transform back to belite (C2S) and free lime, which can lead to decreased compressive strength in the final product as well as problematic setting of the produced cement. [5]

After the cooler, or in some plants within the cooler, the cement clinker is ground to a uniform particle size. Gypsum and other additives are then added in the grinding mill. Finally, the produced cement can be stored in e.g. a silo before being transported to the customer. The storage time is limited due to cement clinker not being a stable material, since it can react with water and carbon dioxide which can result in pre-hydration and carbonation leading to solidification of the material. [5] [8]

2.1.1 Process at site in Slite

This work was based on Cementas production plant in Slite, situated on the island of Gotland in Sweden. Their process, focusing on system line 8, will be described below. The information presented in this section was provided by employees at Cementa [9].

Limestone is mined from a quarry in the vicinity of the site in Slite. The material is transported to a crusher and is mixed with sand and clay, see Table 2.1 for material composition [7]. After being ground further the material is transported via a conveyor to the cyclone tower, also called preheat tower.

Table 2.1: Raw meal composition at Cementa, Slite, January-April 2004 [7]

Raw Material	Composition [%]
Limestone	54.8
Sand	6.0
Marl	37.5
Iron ore	0.3
Fly ash/slag	1.4

The preheat tower consists of two parallel cyclone towers. Both towers start with a double cyclone which is followed by three cyclones in series before the meal enters a calciner and lastly the final cyclone before entering the rotary kiln, see Figure 2.2. Meal is divided by a meal scale into streams entering the two parallel towers, beginning with a double cyclone. Meal enters below the double cyclones and is swirled up into the cyclones with gas exiting cyclone 4. This gas-meal transport results in a highly effective heat transfer due to the large heat transfer area between the small meal particles and the hot flue gases. Meal exits the cyclones at the bottom and enters below cyclone 4 and the same procedure occurs for all the cyclones.

Raw meal exiting cyclone 2, however, enters the calciner where it is mixed with tertiary air from the cooler at entry, which results in a swirling motion along the wall of the calciner see Figure 2.3. This wall of swirling raw meal is heated by a flame located at the top of the calciner. The wall of raw meal also works as heat insulation, ensuring that the vessel wall is not damaged. The fuel used is a mixture of coal and shredded tires, requiring an outlet temperature of 850°C for sufficient burnout. Poor burnout results in high CO levels and energy losses. The meal and gas exiting the two calciners is mixed with flue gases from the rotary kiln. The mixture enters a final cyclone where hot meal is separated from the gas and falls into the rotary kiln. The velocity of the flue gases exiting the kiln needs to be increased before mixing with the flow from the calciners to ensure that the meal does not fall down into the kiln. This is done by what is called a diaphragm, seen in Figure 2.2, that decreases the cross-sectional area of the flow.

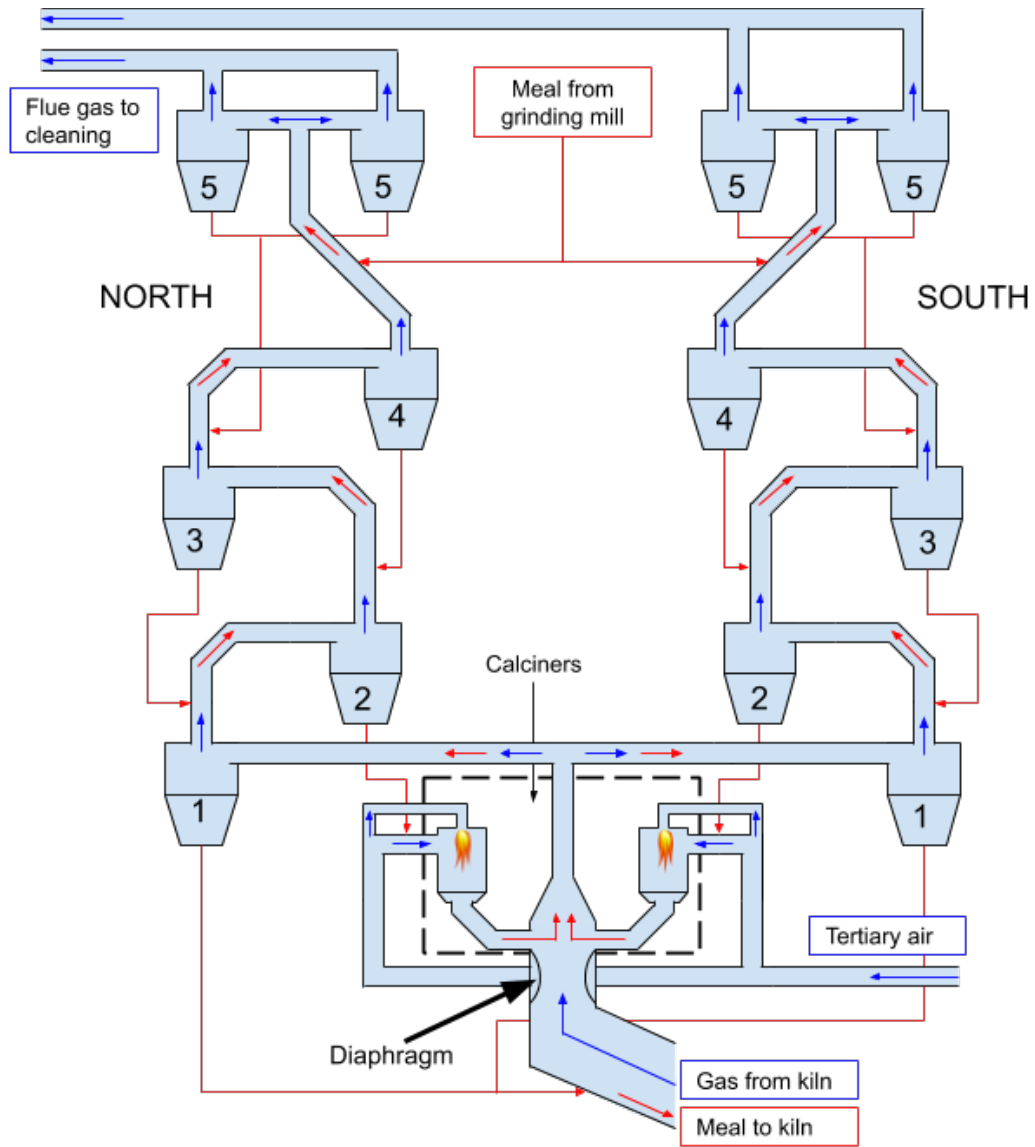


Figure 2.2: Flow sheet of cyclone tower and calciners of system 8 at Cementa, Slite

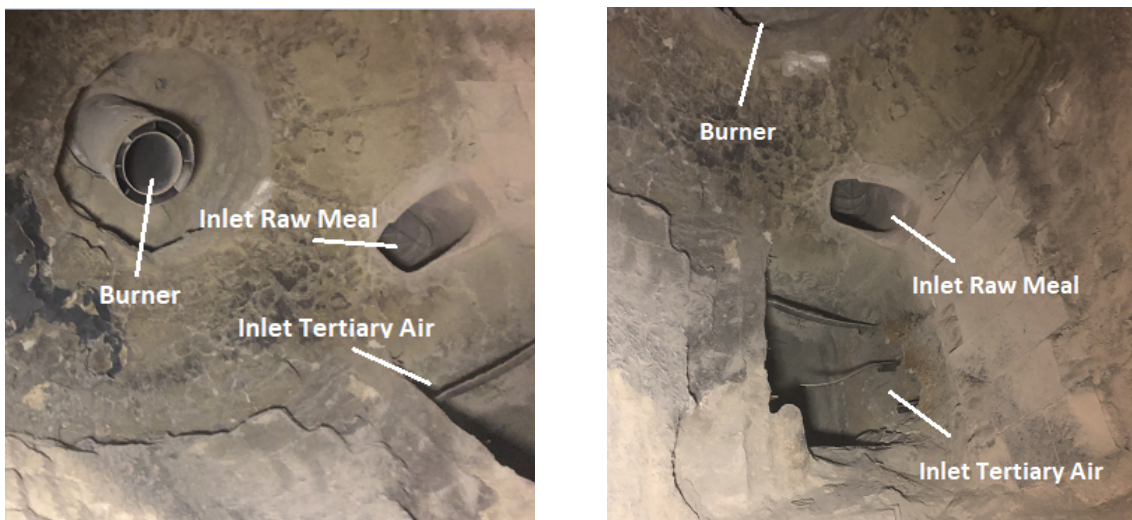


Figure 2.3: Pictures of calciner showing inlet of gas, raw meal and flame

Meal is then fed to the rotary kiln together with a stream of metallurgical slag, which is a by-product from metallurgical industry. The calcination degree (94%) of the hot meal entering the kiln is higher than normal for a system like this, due to the high temperature of the gas exiting the kiln. Higher temperatures, which can be reached once the highly endothermic calcination is finished, will create problems with clogging of meal in the cyclone tower, and is the main reason for stopping at this calcination degree. However, if too much non-calcinated meal enters the kiln the clinker reactions can be delayed which leads to an increased energy need in the kiln due to the need for stressing the clinker formation. [1] See Table 2.2 for the meal composition after calcination.

Table 2.2: Composition of materials in raw meal, after calcination. LOI is the amount of mass lost due to calcination. [7]

Raw Material	Composition [%]									
	CaO	SiO ₂	Al ₂ O ₃	Fe ₂ O ₃	MgO	K ₂ O	Na ₂ O	SO ₃	Cl	LOI
Limestone	50.30	5.25	1.80	0.90	1.00	0.55	0.17	0.70	0.03	39.70
Marl	42.30	14.45	3.39	1.56	2.82	1.07	0.20	1.16	0.02	34.2
Sand	0	96.5	0	0	0	0	0	0	0	0.2
Iron ore	0.20	0.70	0.30	93.70	0.50	0.02	0.03	0.03	0.01	0.1
Fly ash	6.60	46.10	23.00	5.50	1.80	2.06	0.62	1.36	0	12.9

In the kiln, the hot meal is heated to about 1450°C by a flame with the burner positioned at the lower end of the 80 m long kiln, see Figure 2.4. The fuel mixture used in the kiln burner is a mixture mainly between coal and so-called "Fluff". The kiln is declining slightly and rotates by approximately 3.7 rpm to ensure good mixing and forward motion of the material. The second half of the kiln is cooled from the outside using air flows, see Figure 2.5, to prevent the metal from becoming too hot. The inside of the kiln is lined with bricks which work as a heat shield, protecting the metal from the hot meal and gases inside the kiln. As the meal moves through the kiln, more and more clinker sticks to the brick layer. Eventually it comes off and pulls parts of the brick with it, see Figure 2.6, making it a part of the end-product. Towards the end of the kiln, this layer of meal on the bricks can be up to 1 m thick after a year of production.

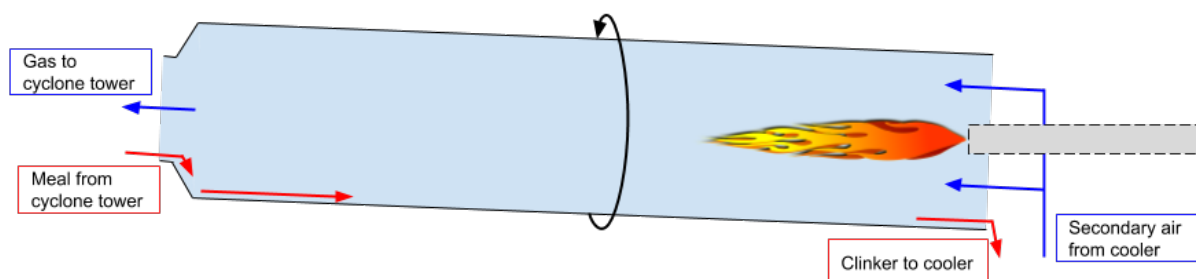


Figure 2.4: Schematic picture of the rotary kiln



Figure 2.5: Picture of cooling air flow nozzle on the outside of the kiln



Figure 2.6: Picture of how parts of the brick lining is pulled off

Hot meal exiting the kiln falls into a grate cooler where it is cooled by air flowing through the meal from below, see Figure 2.7. The air flows come from a number of sections below the grates to ensure an even distribution of air flow and cooling of the material. The hot meal is moved forward by the line of grates, where every second one is moving and the rest are static, see Figure 2.8. About half way through the cooler gypsum is sprayed onto the meal from nozzles in the cooler roof, see Figure 2.9. After the primary cooler, hot meal is dropped onto rotating crushers, see Figure 2.10, grinding lumps as big as 40 cm in diameter, into more evenly sized particles. After the crushers, meal is dropped onto rosters pushing it through a second smaller cooler, where it is cooled further before being ground into product specific sizes and stored in silos.

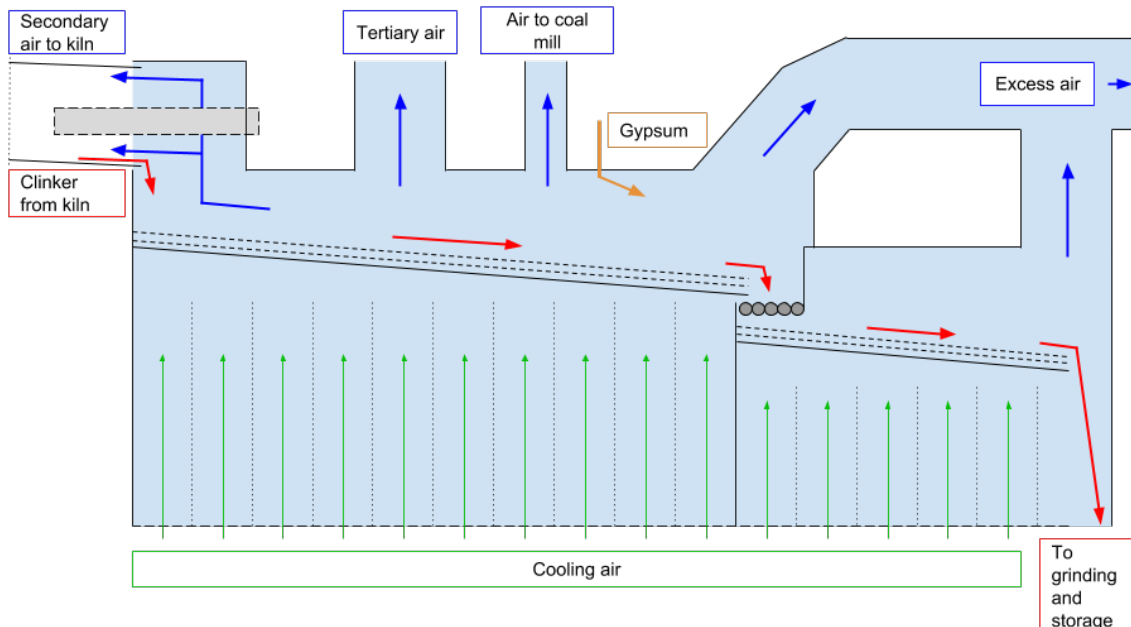


Figure 2.7: Flow sheet of cooler, showing the different flows of air, clinker and gypsum.

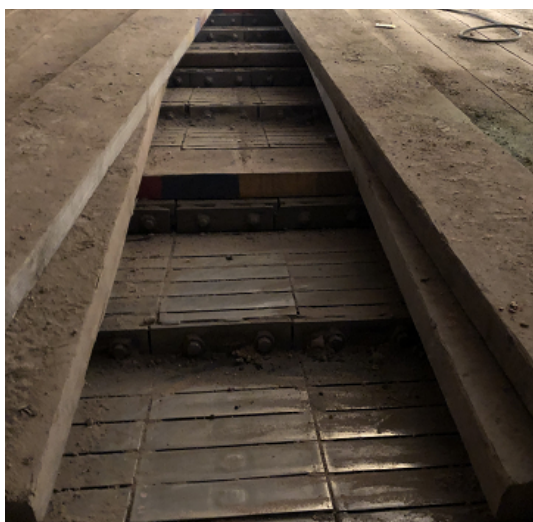


Figure 2.8: Picture of roster rows in cooler



Figure 2.9: Picture of nozzle spraying in gypsum in cooler

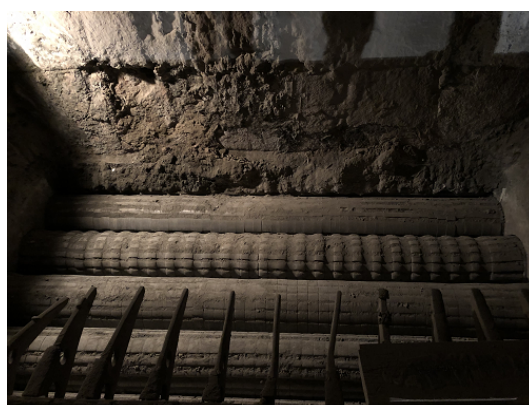


Figure 2.10: Picture of crushers in primary cooler

The process is controlled towards a free lime content of 1.5-2%. Higher concentrations indicates that not enough alite has been produced, or that the raw meal contains too much calcium oxide, which is non-desirable as it decreases the quality of the cement. The free lime in the finished cement product reacts slowly with water creating slaked lime which causes the volume to double. This reaction occurs after the concrete is set and given an excessive free lime content this expansion can cause damages to the concrete and decrease its strength. Having too little free lime is, however, neither desirable. Burning the clinker too hard, to reduce free lime, can lead to sintering of the clinker towards a molten state. This kind of clinker has larger crystals of alite and belite and is therefore harder to grind and requires more energy. Grinding larger crystals causes more electrostatic forces and increases the risk of the crystals agglomerating. Larger crystals also decrease the reactivity of the cement which reduces its strength and increases the setting time. Another reason for keeping the free lime content above $1.5 \pm 0.5\%$ is that it has a stimulating effect on the forming of alite, which leads to higher strength of the material. To control the free lime content the composition of the raw material and how much fuel is burnt in the burners can be varied.

2.2 Plasma Torches

Plasma is often called "the fourth matter of state" and is a state of ionised gas which is generated through heating a gas enough to make its atoms collide and knock off electrons. Plasmas are typically generated by applying an electric current through a gas. [10] In general, plasma consists of electrons, ions and neutral species, which results in the overall plasma being quasi-neutral. [11][12]

Industrial plasmas can be divided into two categories, thermal and non-equilibrium plasmas. Thermal plasmas are characterised by high enthalpy content and temperatures between 2,000-200,000°C. Non-equilibrium plasmas are low-pressure and are characterised by high electron temperatures but low ion and neutral particle temperatures. [13]

A thermal plasma is the relevant option for the application examined in this thesis. They are generated using plasma torches, in which a gas is heated, most commonly by an electric arc. Electric arcs, which are self-sustaining discharges established between an anode and a cathode, are a highly turbulent phenomenon and can be extinguished if disturbed from equilibrium. To keep the arc in steady state it needs to be stabilised, meaning boundary conditions should be created and maintained. A plasma torch stabilises the arc through constricting it, defining its path and cooling the outer layers. The most common technique to stabilise the arc is gas-flow stabilisation, where an external cold layer of flowing gas surrounds the arc column, in either a vortex or an axial flow. A plasma torch can be operated in a transferred or non-transferred arc mode. In a non-transferred mode, both anode and cathode are part of the plasma torch while in a transferred plasma torch the electric arc is established between the torch and the work piece e.g. during welding. [13]

A simple scheme of a plasma torch is shown in Figure 2.11, courtesy of Cambridge International Science Publishing Ltd (CISP). As can be seen in the figure, the plasma torch consists of the internal electrode, 1, the output electrode, 2, and the insulator between the electrodes, 3, through which the working gas, G, enters the plasma torch. The electric arc, 4, is ignited between the two electrodes. Some of the working gas, G_1 , penetrates the arc column while the remaining gas, G_2 , flows between the arc and the wall. [14]

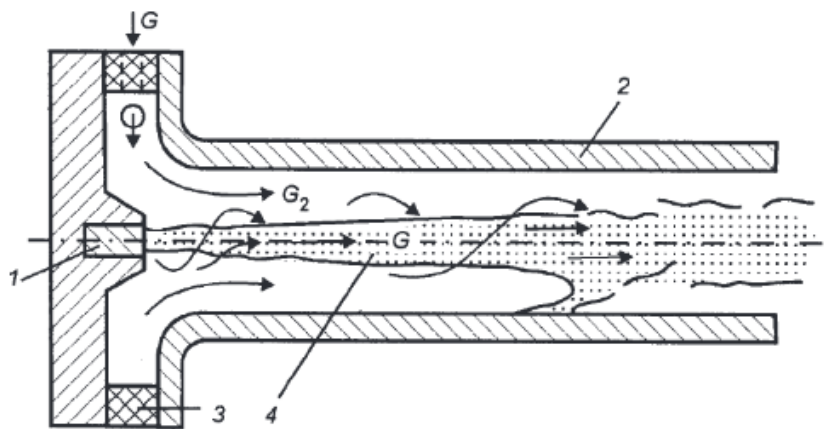


Figure 2.11: Scheme of linear single-chamber plasma torch with self-setting arc length. (1) Internal electrode, (2) Output electrode, (3) Insulator, (4) Electric arc, (G) Working gas, (G_1) Working gas penetrating arc column, (G_2) Remaining working gas [13]

The working gas flow which penetrates the arc column reaches the temperature of the arc through Joule heating. [14] Joule heating, also known as Ohmic or resistive heating, is described as the heat generated when an electric current passes through a resistance. [15] The gas is partially ionised and becomes electrically conductive. The rest of the working gas is not heated much since there is no convective heat exchange with the arc due to a thermal boundary layer "blocking" the heat exchange. Where the wall and thermal boundary layers come together, called the shunting zone, the arc and the main gas flow starts interacting, creating intense mixing of the hot and cold gas flows. This results in a plasma flow with a high-temperature core and rapidly decreasing temperature profile in radial direction forming at the exit of the plasma torch. Less than half of the flow participates in the arc discharge and reaches the plasma state, but it is enough to create and maintain the heating element. The remainder of the gas is heated by the plasma via all three mechanisms of heat transfer. Water cooling of the output electrode is used to minimise the rate of vaporisation of electrode materials due to very high temperatures. [12]

The choice of gas in a plasma torch is mainly based on gas enthalpy, reactivity and cost. The most common gases are argon, helium, nitrogen, air and hydrogen. To get a stable arc, the plasma gas flow rate and the electric power supplied to the plasma torch must be balanced. The gas flow must be controlled to make sure it does not blow out the arc, but is large enough to be able to push the arc through the nozzle. [13]

Plasma torches have various industrial applications within mechanical, chemical and metallurgical processing. Several applications are mentioned in literature, including: cutting and welding, evaporation, refining, surface treatment, gas-heating, plasma synthesis, sintering, fine-powder preparation and plasma waste-treatment. [13]

Today, the maximum power of a plasma torch in industry is 8 MW with a typical efficiency of 85-90%. [1] Typical data for an 8 MW plasma torch was provided by ScanArc and is presented in Table 2.3. According to ScanArc, CO₂ is a very good choice of working gas for plasma torches.

Table 2.3: Plasma torch data provided by ScanArc [16]

Parameter	Value
Effect	8 MW
Volumetric flow	2285 Nm ³ /h
Temperature	2500-3500 °C

An advantage of replacing conventional burners with plasma torches, other than decreased greenhouse gas emissions from replacing combustion, is that the operating costs can decrease, according to a comparison performed by L. Rao, F. Rivard and P. Carabin [17] on a 2 MW fuel oil burner and a 2 MW air plasma torch. They state several reasons why the operating costs are lower, including decreased costs of heat production due to fuel consumption being replaced by cheaper electricity. Secondly, no more handling and extraction of fuels would be necessary, meaning less process equipment utilisation and manpower. Thirdly the volumetric flow of gas could decrease which means that the cost of off-gas treatment decreases.

The amount of off-gas can decrease with up to 80% compared to the off-gas amount from using conventional burners. [17] The decreased amount of gas would also have downsides, mainly a decreased convection contribution, although the increased temperatures of the flame could lead to increased radiation, if the gas used is radiant. However, particles have large radiative characteristics and are a large contribution to the radiation of a flame, and particle injections in a plasma can be very difficult due to the high viscosity, which means that the amount of radiation would still possibly decrease due to the lack of particles. Having no combustion will lead to no ash production and less foreign trace elements exiting the stack, however the ash is used as an additive in the cement, so without it the chemical composition of the raw meal has to be adjusted. [1] A plasma does not contaminate the process environment and therefore ensures a high purity of the product. [18]

2.3 Carbon Capture and Storage

Carbon capture and storage (CCS) refers to capturing CO_2 at some stage in a process, purifying the stream and storing the CO_2 , using one of a few technologies [19]. CCS is a necessity for fulfilling the climate goals of keeping the global average temperature increase below 1.5°C ; CO_2 emissions must start to decrease from 2020, and possibly become negative, making CCS unavoidable if fossil fuels are to be continuously used at a rate of even 10% of today's. [20] Some capturing technologies are: pre-and post-combustion capture, oxy-fuel combustion and chemical looping systems. Pre-combustion capture involves gasifying fuel with sub-stoichiometric amounts of oxygen at elevated pressures to give a 'synthesis gas' mixture of predominantly CO and H_2 . The synthesis gas can then be combusted to give heat and a flue gas stream containing CO_2 and H_2O which is easily separated with condensation. Post-combustion capture involves removing most of the CO_2 from the flue gases after combustion. [21] Oxy-fuel combustion means providing pure oxygen to the combustion rather than air, resulting in a flue gas without nitrogen. Lastly, chemical looping systems are a kind of oxy-fuel technology where oxygen is introduced to the combustion chamber via a metal oxide carrier that is partially or fully reduced during combustion and then re-oxidised in another reactor. [22]

The requirements of the gas composition for storage varies and it is difficult to find specific values for the acceptable compositions. It usually depends on the specifications for the pipelines transporting the gas to storage, however there are some common requirements. The amount of CO_2 should be above 95% while the amount of NO_x , SO_x , HC , H_2S and water vapour must be low, since these compounds can form acids. The amount of O_2 should also be low. [23]

The captured CO_2 is pressurised to around 100 bar before being transported to a storage site. [19] Possible storage options are geologic storage, see Figure 2.12 courtesy of Michael Mann, and ocean storage, where the first option includes using depleted oil and gas reservoirs to store the gas. Studies have shown that using depleted reservoirs for storage of CO_2 stabilises the voids left when removing the oil and gas. The other alternative, ocean storage, could be an option since the ocean is not saturated with CO_2 . [24]

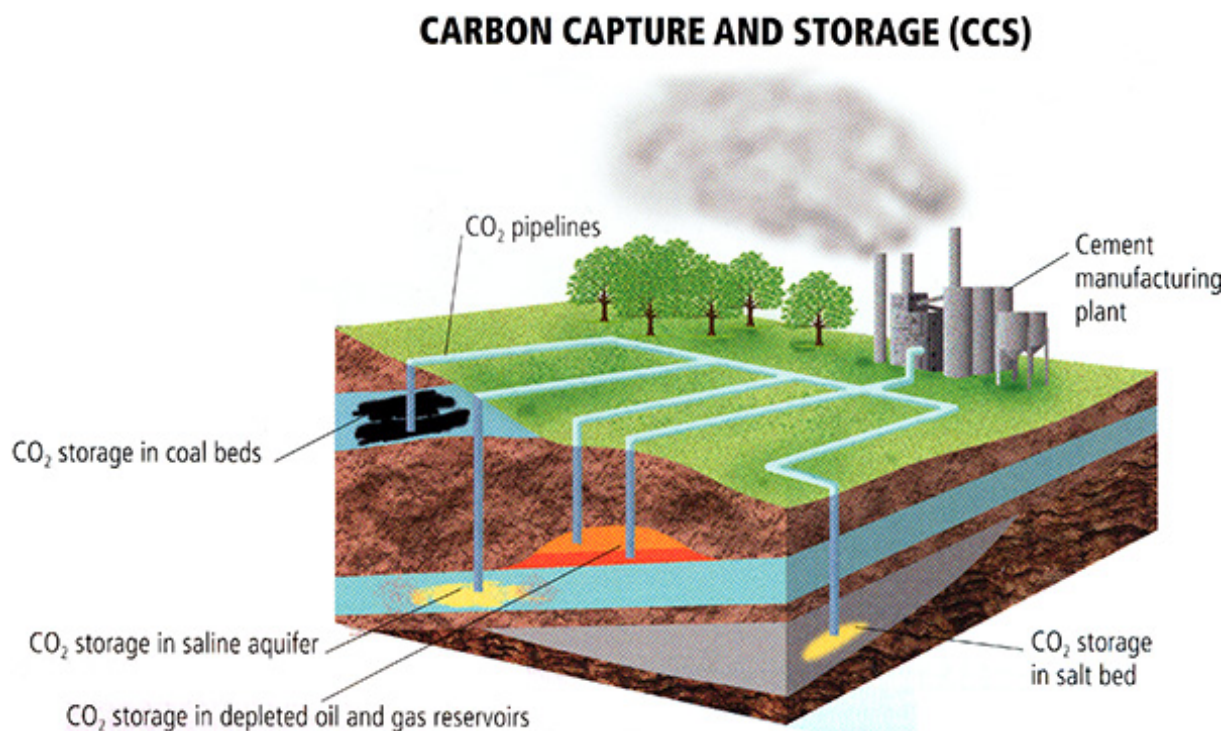


Figure 2.12: CCS in combination with a cement production process [25]

2.4 Implementation of Plasma Torches and Carbon Capture and Storage in Cement Production

Implementing plasma torches in the cement production process could lead to a significant decrease in CO₂ emissions, as well as emissions of other undesired compounds, such as CO, from combustion, and be the first step towards a cement industry free from CO₂ emissions. Making the entire cement industry free from CO₂ emissions from combustion would mean a decrease of 916 Mt CO₂/year, 40% of the total annual emissions. If CCS were to be implemented as well it would mean a decrease of 2.8 Gt CO₂/year.

By removing combustion the produced NO_x from the fuel would be eliminated, but at the high temperatures of the plasma process, NO_x could instead form from nitrogen gas in the air. In order to have no emissions of NO_x, there can be no air leakage since a pure plasma gas without any nitrogen or oxygen is required. Compounds like H₂S and SO_x, would not form either due to them arising from the fuel as well. Therefore gas cleaning would not be necessary, not considering cleaning steps required for CCS, and those operational costs would decrease. However, having no SO_x means that no gypsum can be produced and it will need to be acquired externally.

The preferred working gas of the implemented plasma torches is CO₂. The reason for CO₂ being the preferred working gas is that CO₂ will still be produced from calcination, and to prepare for future implementation of CCS it is desirable to have as pure gas flows as possible. The CO₂ can be acquired by recirculating the CO₂ from calcination, which is another advantage of using CO₂ as working gas.

Before implementing plasma torches in the kiln, some issues would need to be examined. If the kiln should still be connected to the cooler and cyclone tower, and a clean CO_2 flow is desired, then air could not be used in the cooler and combustion would not be possible in the calciners. A solution to this which could be further investigated is implementing a different heat source in the calciners, recirculate CO_2 generated from calcination and cool it for heat and use it in the cooler. The heat generated from cooling the CO_2 before the cooler could be utilised in other parts of the process, such as drying the meal, or elsewhere, to make sure this heat is not lost. The amount of CO_2 generated from the calcination is not enough to cool the material sufficiently, so there is need for accumulating or acquiring CO_2 until there is enough, and then the excess amount of CO_2 could be separated, and eventually captured and stored. Another solution could be to disconnect the kiln from the cooler and cyclone tower, so that only the material moves between these. However, this would be difficult to implement, due to the current layout of the system at site. For a pure CO_2 flow, there is need for air tightening the process, since no air leakage would be accepted, meaning that more research on how to successfully make the process air tight needs to be done.

For capturing CO_2 in cement production post-combustion capture and oxy-fuel combustion has been considered previously. To decrease the energy demand for the separation of CO_2 , a gas stream as pure as possible out of the plant should be achieved. [22] Cementa is part of HeidelbergCement, that also owns a plant in Brevik, Norway which is evaluating amine-based carbon capture. The European Cement Research Association has investigated the potential of creating gas tight production by retrofitting existing facilities to enable an oxy-fuel process in the future to simplify carbon capture. Calcium looping and the Leilac-project mentioned above are other concepts of interest for the cement industry and the Group HeidelbergCement. The whole industry is interested in reducing emissions, and agree on CCS being the way to move forward. [1]

The CCS technology considered as addition to plasma torches is post-combustion capture. If plasma torches with CO_2 as working gas are implemented the gas flow would be very clean, and separation of CO_2 would not require as much energy and process steps as it would if another gas was used.

3

Method

The method includes data gathering, overall energy balances and modelling. The modelling was divided into two parts, 1) the meal in the cyclone tower and 2) a heat flux model of the heat transfer mechanisms in the rotary kiln. The heat flux model is described together with the changes made to it for modelling cement production and for plasma modelling.

3.1 Project Method

A schematic image of the working process of the project is shown in Figure 3.1. A literature study initiated the project, providing theory on the related subjects, such as plasma torches, CCS and previous modelling approaches, and information on which parameters would be relevant to include in the model and what could be neglected. The literature study also provided general understanding of the cement production process which was expanded during a site visit where data was gathered. The data-collecting period at Cementa's largest cement production plant in Slite provided information on the plant and the production, as well as operational data of the current process. This data was used as basis and validation of the models. Employees at Cementa were involved during the project, assisting with experience and knowledge of the process. See Section 3.3 for how data was handled.

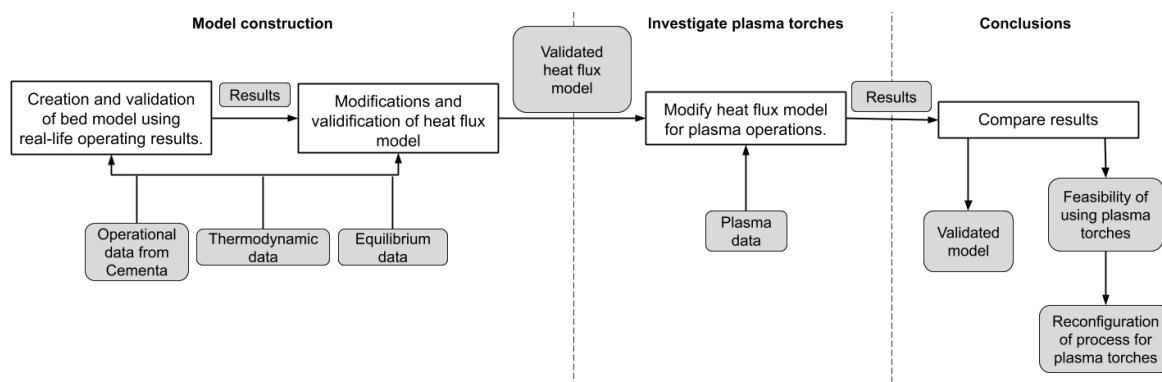


Figure 3.1: An overview of the method for this thesis

The meal modelling was done in three parts described in Sections 3.3.2 and 3.4, where the first was used to calculate overall energy need in the cement production process, the second was an iterative model, hereafter referred to as "bed model", that solves energy balances in the cyclone tower and the third a heat transfer model over the rotary kiln.

The models were developed in Matlab combined with FactSageTM data to account for the equilibrium dependency. The bed model is an iterative model solving energy balances using modified equilibrium data to account for equilibrium not being reached at all specific temperatures and it does not include specific reactions. The results of this model were compared with the gathered operational data to validate the model. Results were then used as input data for the heat flux model over the rotary kiln. This model, hereafter referred to as "heat flux model", described the rotary kiln and the heat transfer within it. The model has previously been used to describe rotary kilns in the iron ore pelletising industry and was modified to simulate the current process of heating clinker with a coal burner. In this work, the model was used to calculate the heat absorbed by the hot meal in the rotary kiln. How the heat flux model was modified and alternated for this process is described in Section 3.5. The resulting product temperature was compared with gathered process data to validate the model.

Once the models were validated for the current process, the heat flux model was modified to represent heat transfer from a plasma torch. How the heat flux model was alternated for the plasma modelling is described in Section 3.5.1.

3.2 Equilibrium Data

Equilibrium data for the species relevant to cement production was extracted from FactSageTM. It was extracted as a matrix of equilibrium compositions in grams at temperatures from 50°C to 1750°C, based on the total mass flow and inlet composition of material. The mass fraction of each specie at every temperature was calculated from the flow. A fraction was also created to account for the change in the total mass flow from the inlet mass flow, i.e. at 50°C. This is due to CO₂ leaving the solid phase and thereby decreasing the total mass flow of meal, which needs to be taken into account.

The compositions used as indata in FactSageTM were calculated from the raw meal compositions found in Table 2.1 and 2.2, but excluding MgO, K₂O, Na₂O, SO₃ and Cl for simplification. The amount of CaCO₃ entering the cyclone tower was calculated from the calculated amount CaO, using Equation 3.1, and the mass of CaO was then set to zero.

$$m_{\text{CaCO}_3} = m_{\text{CaO}} \frac{M_{\text{CaCO}_3}}{M_{\text{CaO}}} \quad (3.1)$$

Some modifications were made to the equilibrium data. If all species in the raw meal are introduced in FactSageTM at 50°C several reactions occur. Any produced CaO reacts with SiO₂ to form calcium silicates instead of existing as free lime. This is not consistent with what happens according to theory on cement production. One reason for this could be that in FactSageTM ideal conditions for reactions are assumed, with regards to mixing

and contact between species. In reality the meal in the cyclone tower swirls around while mixing with gas which makes reactions between species difficult to achieve. To make the equilibrium data resemble reality, the matrix was modified so that no reactions occur before 900°C, but calcination between 700-900°C. Furthermore, the data was changed so that the calcination degree at 850°C, inlet temperature of the kiln, was set to 94% instead of 100%. Equilibrium data was gathered from 1000-1750°C with all reactants present, and allowing all possible products according to FactSageTM. The data for the two temperature intervals was then combined by making a linear approximation between 900-1000°C. In the kiln, all species of the meal are considered to come in contact since it's well mixed, which means that the equilibrium data in the temperature range of the kiln could be assumed consistent with cement production theory.

The only part not included in the data from FactSageTM was a melted phase, SLAGA, which was added manually [7]. The melted phase consists of the species containing aluminium and iron. In this case the tetracalcium aluminate and ferrite oxide. Ferrite oxide originated from C2F and releases CaO which then reacts with C2S to form C3S. According to data from Cementa and other sources [26], the melted phase begins forming around 1350°C and all metals are fully melted at 1400°C. To create the melted phase, the mass of all species containing aluminium and iron was set to zero at 1400°C and the mass of the melted phase was set as the total mass reduction of C3A plus the mass of Fe₂O₃ from C2F. Molar balances were performed for all species in the system.

3.2.1 Thermophysical Data

Temperature dependent specific heat capacities were received from Cementa for the species available in FactSageTM. To include heat of reaction in the process, which is an important heat source and sink, heat of formation for each specie was gathered. Since the reaction paths are not treated, this was a way of including the heat of reaction and is further explained in Section 3.3.2.

3.3 Reference case

Below follows a description on how data used in the model construction was gathered. Some data was received from Cementa while some were extracted from the software FactSageTM. The rest of the needed data was found in encyclopedias and reports. This is followed by a calculation on the total energy need of the process based on this data and the equilibrium data described previously. The results from this calculation are used as a reference for further modelling of the process.

3.3.1 Cementa Data

During the data-gathering period at the plant in Slite, a review of the plant with tours of the area, both during production and at full stop, was performed. Photos used in the

report were taken during the latter of the tours at the time for the yearly stop of the process. Access was granted to their document system including drawings of cyclones and calciner as well as flow sheets of the relevant parts. Also access to their process data through IP21 was granted, where live data and historical trends for temperatures, flow etc. could be extracted. To determine what data would be useful, the extracted flow sheets were studied together with operational staff to get a better understanding of meal and gas flow through the process. With better understanding of the process flows, flow and temperature meters could be selected from which data should be extracted.

To have multiple operational cases to validate the models with, data from two 10 day periods were extracted, hereafter denoted as operational case 1 and 2. To decide which periods would be suitable, key parameters as material feed, fuel consumption and free lime content were compared and trends were evaluated to find 10 day periods with stable production. Due to the Swedish climate differing along the seasons, 2 operational cases were found to be appropriate: one during fall and one during winter, so that the outside temperature could be taken into account. Difference between the two operational cases were mass flows of meal, temperatures and volumetric flows of gas. To handle outliers in the data, the maximum and minimum values were compared with the average for each dataset. If the difference was larger than 50% the values were considered outliers, and were removed if it was deemed necessary.

Data extracted from IP21:

- Temperatures
- Gas flows
- Material flows
- Rotational speed of the kiln
- Meal splitting between cyclone towers
- Heat consumption in kiln and calciners

3.3.2 Overall Energy Balance

Before developing a process model, an energy balance of the whole process as a black box was done to see if the energy input to the real system at Slite would be sufficient to heat the meal when including the reaction heat and heating of the gas. The total need for heating the meal was calculated by comparing the energy content of the meal before and after the cyclone tower and kiln, see Equation 3.2. The change in heat content of the gas was calculated by Equation 3.3. The exiting gas mass flow has increased compared with the inlet mass flow due to released CO_2 from calcination and addition of tertiary air.

The total heat of reactions was calculated by comparing the mass flow of species at the inlet and outlet and multiplying the difference in mass flows with each species respective heat of formation, see Equation 3.4. If Q_{react} is positive, the total sum of reaction heat is endothermic while if it is negative it is exothermic. These calculations were made both on the whole process and on the cyclone tower and kiln separately. By doing this the amount of heat needed in the respective parts could be calculated, see Equation 3.5. This value could then be compared to the amount of heat added in different parts of the process according to process data.

$$Q_b = H_{b,out} - H_{b,in} = \sum (\dot{m}_i c_{p,i} T)_{b,out} - \sum (\dot{m}_i c_{p,i} T)_{b,in} \quad (3.2)$$

$$Q_g = H_{g,out} - H_{g,in} = (\dot{m} c_p T)_{g,out} - (\dot{m} c_p T)_{g,in} \quad (3.3)$$

$$Q_{react} = \sum_i (m_i(T_{out}) - m_i(T_{in})) h_{f,i} \quad (3.4)$$

$$Q_{need} = Q_b + Q_g + Q_{react} \quad (3.5)$$

3.4 The Bed Model

In this section the bed model written in Matlab for the cyclones and calciners is described. The two parts are modelled similarly but with the following key differences: The model created for the cyclones and calciners solves heat balances for the meal, which is counter-current with the gas flow in all parts except for the calciners. Since no specific reactions are modelled and the equilibrium data is not time dependent, time was not considered as a parameter. The difference in out- and inlet mass flows of all species in every cell determined the reaction heat produced or consumed based on heat of formation of the species, see Equation 3.4.

Densities of solid species in the model were assumed to be constant and since the particles are ground to fine powder, conductive heat transfer is neglected. Perfect mixing for both the gas and bed was assumed in the cyclones and calciners, and is solved only in axial direction. Steady-state was assumed as well as neglecting any momentum impact the gas might have on the meal, mainly in the cyclones and calciners. The loss of meal dust due to gas momentum impact is instead put as a 15% loss of input flow at the first cyclone.

3.4.1 Cyclones

The cyclones are modelled as open heat exchangers, solving the energy balance for each cyclone by Equation 3.6. To solve this equation, an outlet meal temperature is guessed to calculate $H_{b,in}$ and $H_{b,out}$ from Equation 3.2 and Q_{react} from Equation 3.4. Figure 3.2 shows the temperatures and mass flows used in the energy balance. The outgoing temperature and mass flow of the meal are solved while the other parameters shown in the figure are known from process data. Due to calcination, carbon dioxide is released in the cyclones, which means the mass flow of the meal decreases and this is taken into account by the fraction created in the equilibrium data, see Section 3.2. The outgoing temperature of the released CO₂ was assumed to be equal to the outgoing gas temperature.

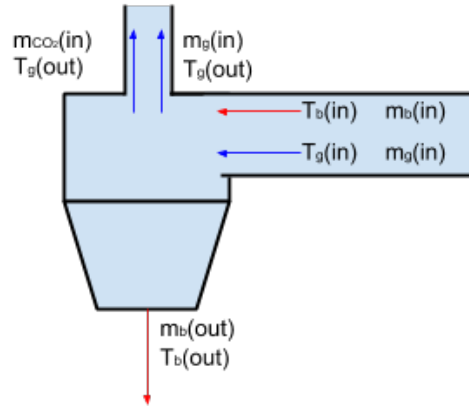


Figure 3.2: Temperatures and mass flows used in modelling of cyclones

The heat content of the entering and exiting gas is calculated using its inlet and outlet temperature, see Equation 3.7. The heat content of CO_2 exiting the cyclone is calculated using Equation 3.8. The properties of all gases are approximated to those of air for simplicity. If the difference in the energy balance is lower than 0.005 MW, the outlet temperature and composition are used as the inlet values for the next cyclone. If not, a new, slightly higher temperature, is tested, and the same calculations are repeated.

$$H_{b,in} + H_{g,in} + H_{\text{CO}_2,in} = H_{b,out} + H_{g,out} + H_{\text{CO}_2,out} + Q_{\text{react}} \quad (3.6)$$

$$\begin{aligned} H_{g,in} &= \dot{m}_{g,in} c_{p,g} T_{g,in} \\ H_{g,out} &= \dot{m}_{g,in} c_{p,g} T_{g,out} \end{aligned} \quad (3.7)$$

$$\begin{aligned} H_{\text{CO}_2,in} &= 0 \\ H_{\text{CO}_2,out} &= \dot{m}_{\text{CO}_2,out} c_{p,g} T_{g,out} \end{aligned} \quad (3.8)$$

3.4.2 Calciner

In the calciner, the gas and mass flows are co-current. The two parallel calciners were modelled as open heat exchangers similar to the cyclones, and the energy balance in Equation 3.9 is solved to find the exiting temperature of the meal. The difference between the cyclone model and calciner model is that the heat addition was modelled as two terms in the calciners; the heat loss of the gas from Equation 3.7 and the combustion occurring in the calciner. Q_b and Q_{react} in the energy balance were calculated by Equations 3.4 and 3.2. The temperature of the exiting gas was set to be equal to the temperature of the exiting meal. The amount of heat received from combustion was calculated using the fuel input and an efficiency set to 95%.

$$0.95 \cdot Q_{\text{comb}} + H_{b,in} + H_{g,in} + H_{\text{CO}_2,in} = H_{b,out} + H_{g,out} + H_{\text{CO}_2,out} + Q_{\text{react}} \quad (3.9)$$

The mixing point between the gas flows from the calciners and the kiln can be seen in Figure 3.3. All temperatures in the figure are known except T_{kiln} which was calculated by solving Equation 3.10 from H_{kiln} . The energy content of the gas from the kiln was found through solving Equation 3.11, see Equations 3.12, 3.13 and 3.4 for how the components were calculated. This heat exchange occurs from the mixing point until the hot meal and gases are separated in the last cyclone, which is why the last cyclone is not modelled separately.

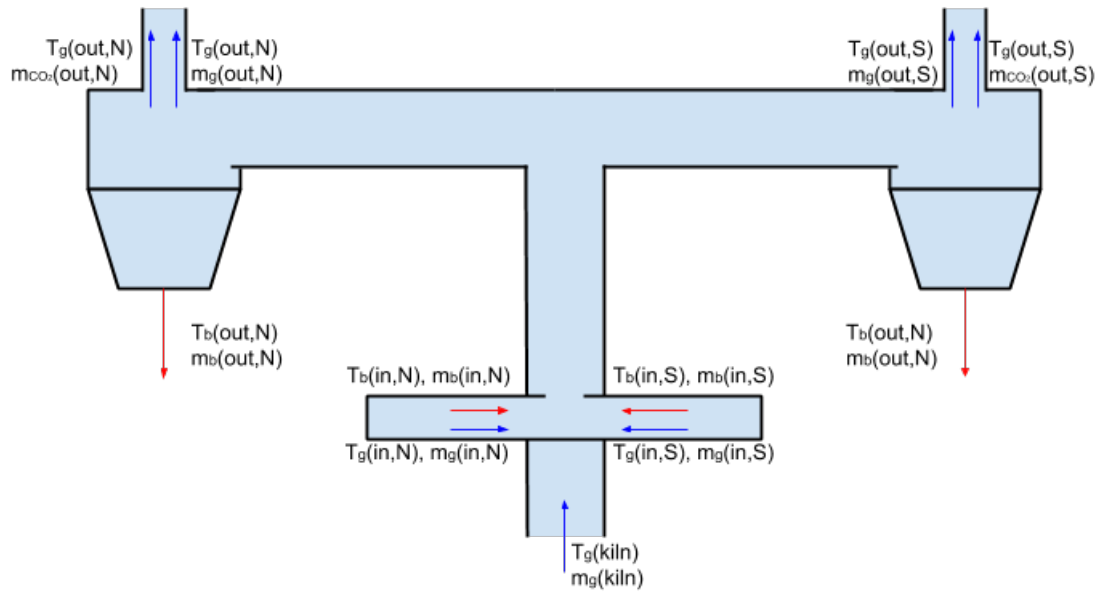


Figure 3.3: Mixing point after calciners

$$H_{kiln} = (\dot{m}_g c_{p,g} T)_{kiln} \quad (3.10)$$

$$H_{g,out} + H_{b,out} + H_{CO_2,out} + Q_{react} = H_{g,in} + H_{b,in} + H_{CO_2,in} + H_{kiln} \quad (3.11)$$

$$\begin{aligned} H_{g,in} &= (\dot{m}_g c_{p,g} T_g)_{in,N} + (\dot{m}_g c_{p,g} T_g)_{in,S} \\ H_{g,out} &= (\dot{m}_g c_{p,g} T_g)_{out,N} + (\dot{m}_g c_{p,g} T_g)_{out,S} \end{aligned} \quad (3.12)$$

$$\begin{aligned} H_{b,in} &= (\dot{m}_b c_{p,b} T_b)_{in,N} + (\dot{m}_b c_{p,b} T_b)_{in,S} \\ H_{b,out} &= (\dot{m}_b c_{p,b} T_b)_{out,N} + (\dot{m}_b c_{p,b} T_b)_{out,S} \end{aligned} \quad (3.13)$$

3.5 Heat Flux Model

The heat flux model was provided from a Chalmers project in cooperation with LKAB. The model describes heat transfer in a rotary kiln where the bed material is heated by radiation from a flame, hot gases and the surrounding wall. The wall is also heated by radiation and further provides heat to the bed by conduction within bed and from the wall. Losses to the environment outside the kiln are included. As the kiln rotates, meal slides axially towards the lower part of it, while, due to tumbling, meal is transported to higher parts of the kiln, falls over and mixes into the bigger bulk. The bed is divided into a bottom and a surface layer as shown in Figure 3.4, where the bottom layer is subject to the heat conduction from the wall. [27]

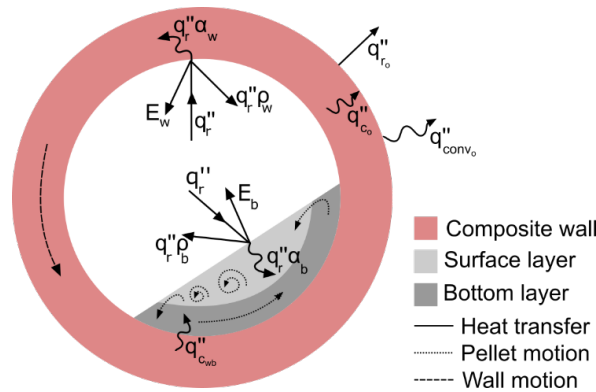


Figure 3.4: Cross-section of a rotary kiln shown different possible heat exchanges occurring, as well as movement, mixing and rotation [27]

The kiln volume is divided in cells in the radial, axial and angular direction and a flux profile is calculated based on a set temperature profile of the gas, amongst other parameters. The radiative heat transfer equation is solved using a discrete-ordinates method and radiative properties are calculated using a weighted sum of grey gases model. Particle properties are calculated using Mie and Rayleigh theory. The bed and wall temperature profiles are solved through iterations based on an initial guess. [27]

To model the current cement production case, some alterations needed to be made in the model. Temperature dependent heat capacities were added where only a single constant value was used earlier. These heat capacities are the same as those used in the bed model, and they were added together with the mass fraction equilibrium data. Convective heat transfer between gas and bed was also added, see Equations 3.14 and 3.15. [28] Moreover, data in the model were changed to fit operational cases gathered in Slite.

$$G_g = \frac{\dot{V}_g \rho_g}{A_{cs}} \quad (3.14)$$

$$q''_{conv} = h_{cv} (T_g - T_b) = 0.4 G_g^{(0.62)} (T_g - T_b) \quad (3.15)$$

Due to the complexity of the model and the strongly, partly exothermic and partly endothermic, reactions, including heat of reaction in the iterations as done in Section 3.4.1 was not a suitable option. Heat of reactions was instead added to the model as source terms by introducing seven reaction zones (Z1-Z7), shown in Figure 4.3, into the kiln. This was done by dividing the length of the kiln into seven zones, see Figure 3.5. Here, it is considered that the calcination occurs in the first zone, the formation of C2S in the second zone, formation of C3S in the fourth zone, formation of SLAGA in the sixth zone and no reactions occurs in the third, fifth or seventh zones. The length of each zone was dependent on the temperature increase in the specific zone and knowledge on how fast reactions like the calcination are. The reaction heat of all zones for both operational cases are presented in Table 4.4.

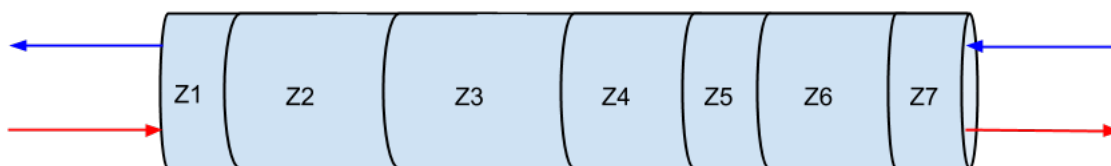


Figure 3.5: Illustration of zones created in the rotary kiln of the heat flux model

Modelling of the combustion reactions is not included in the model. In other words, an effect of the burner can not be put into the model to receive resulting temperature profiles of gas and bed. The gas profile is instead set as an input, created based on previous measurements of coal flames in an iron pellet rotary kiln. Data used in the heat flux model are presented in Table 3.1, where flame temperature and length was received from Cementa. The contact factor is a guessed value describing how much of the bed surface is in direct contact with the wall. The flame temperature is higher than the adiabatic flame temperature of a coal flame, and it is noted that this is a very high value. However, it was set this high due to information received by Cementa as well as the necessity of reaching the correct product temperature of the meal. Since it is difficult to measure the temperature profile in the kiln, guesses of its appearance had to be made. This is a large source of uncertainty in the model and the produced results.

Table 3.1: Parameters for heat flux model

Parameter	Value
Maximum Flame Temperature	2100 °C
Flame length	25 m
Radius	2.1 m
Maximum flame radius	2.05 m
Flame radius at burner	1.52 m
Emissivity of wall	0.75
Emissivity of bed	0.90
Density of bed	1450 kg/m ³
Contact factor	0.4

The radius is set lower than the actual radius of 2.6 m to compensate for the build up of meal attaching gradually to the layer of bricks towards the end of the kiln. The layer of clinker at the far end of the rotary kiln is 1 m and therefore the radius of the kiln is decreased by 0.5 m, and a layer of clinker with a thickness of 0.5 m is added to the wall. Thicknesses and heat conductivity for the layers of the kiln wall are listed in Table 3.2.

Table 3.2: Parameters for kiln wall in heat flux model

Parameter	Value
Clinker layer	0.5 m
Clinker conductivity	0.5 W/mK
Brick layer	0.32 m
Brick conductivity	0.15 W/mK
Steel layer	0.05 m
Steel conductivity	80.4 W/mK

Grid independence was checked for, by running the model for operational case 1 data for different grid resolutions. Radial cell discretisations between 6-14 were tested and axial cell discretisations between 10-200 were tested. The angular cell discretisation was set so the bed angle would be 1.57 radians, which corresponds to an 8% fill of the kiln. All runs of the model for coal and plasma were hereafter done with the grid size showing accepted grid independence. Sensitivity analysis was made for the parameters contact factor, emissivity of the wall and the bed and lastly the flame temperature.

A limitation of this model is that it is a rather time-consuming model to run, which meant that the resolution of the grid could not be as good as desired at all times. Another limitation was that individual particles in the bed are not modelled, resulting in the mass transfer and reaction heat being independent of the size of particles.

3.5.1 Plasma Modelling

To model plasma torches in the heat flux model, additional alterations had to be made. Gas flow, gas temperatures, amount of particles in the gas and gas composition were modified. The amount of particles were set to zero due to no particles being present in a plasma. The composition of the gas was changed to 87.5% CO₂ and 12.5% H₂O to simulate a CO₂ plasma torch, due to the model not being defined for properties of H₂O/CO₂ ratio of less than 1/8. Data was received from ScanArc on laboratory tests made on plasma torches in cement production. This data was then linearly scaled up in a first attempt. Inputting the heat requirement of the meal and a minimum outlet temperature of the gas gives temperatures and volumetric flow of gas required for different installed effects of plasma torches. Based on the data, the smallest possible installed effect was 65 MW, see Table 3.3 for volumetric flow and temperatures. This effect was the only one tested due to time limit of the project.

Table 3.3: Specifications of plasma torches modelled

Parameter	Value
Effect	65 MW
Gas flow	11304 Nm ³ /h
Gas temperature at inlet, centre	3014 °C
Gas temperature at outlet, centre	949 °C

The gas temperature profile was set in a different way compared to modelling a coal burner. Instead of setting specific temperatures at certain positions in the kiln, the gas temperature profile was created based on the temperature at the centre of the plasma jet and the initial guesses for the wall temperature at the inlet and outlet of the kiln. The axial temperature profile at the centre was set so the gas held a close to constant temperature a few meters into the kiln, simulating a plasma jet and slow mixing with surrounding gas. Then the profile decreased linearly to the outlet temperature. Similarly, the radial temperature profile at the torch end was set close to constant for a distance and decreased linearly to the wall. At all other points in the kiln the radial temperature profile was linear between the temperature in the centre and the wall. The profile was then modified by changing the initial guess of the inlet gas temperature by the wall until a desirable product temperature were reached. The gas temperature profile was the result of this simulation.

The simulations of implementing plasma torches required iteration between the heat flux model and the model for calculating the overall energy need, to find the correct reaction zone values corresponding to the outlet temperature. Using an initial vector for the heat of reaction, the heat flux model was run to get the outgoing clinker temperature. This temperature was then used to calculate a new heat of reaction to put into the heat flux model and repeat the process until the temperatures were the same.

A limitation of modelling plasma torches with this model is, as for when modelling coal burners, that there is no way of putting in a burner effect into the model. The model should be improved to include a model describing the creation of the plasma as well as the plasma jet itself.

4

Results and Discussion

In this chapter the results are presented and discussed. First, the resulting inlet composition and equilibrium data used is presented, followed by results from the overall energy balances. Thereafter temperature results and reaction heat from the bed modelling are presented. Lastly, results from modelling the coal and plasma in the heat flux model are presented.

4.1 Equilibrium Data

The mass compositions into the cyclone tower and into the kiln used in FactSageTM are shown in Table 4.1. The resulting equilibrium data used in the models are shown in Figures 4.1 and 4.2. Finding accurate material data was challenging due to not much being known about the cement chemistry and the reactions occurring in the process. Several adjustments had to be made to the equilibrium data that was extracted to make it resemble theory on cement production. Which reactions occur and when, highly affect the resulting temperature profiles due to the highly endothermic and exothermic zones in the process. The modifications made were motivated by theory and approved by employees at CEMENTA, leading to the material data being assumed to be valid and correctly representing the reaction course in the cyclone tower and kiln.

Table 4.1: Inlet compositions used in FactSageTM

	Inlet mass [kg]				
	CaCO ₃	CaO	SiO ₂	Al ₂ O ₃	Fe ₂ O ₃
Cyclone tower	80.55	0	15.28	2.68	1.48
Kiln	0	45.13	15.28	2.68	1.48

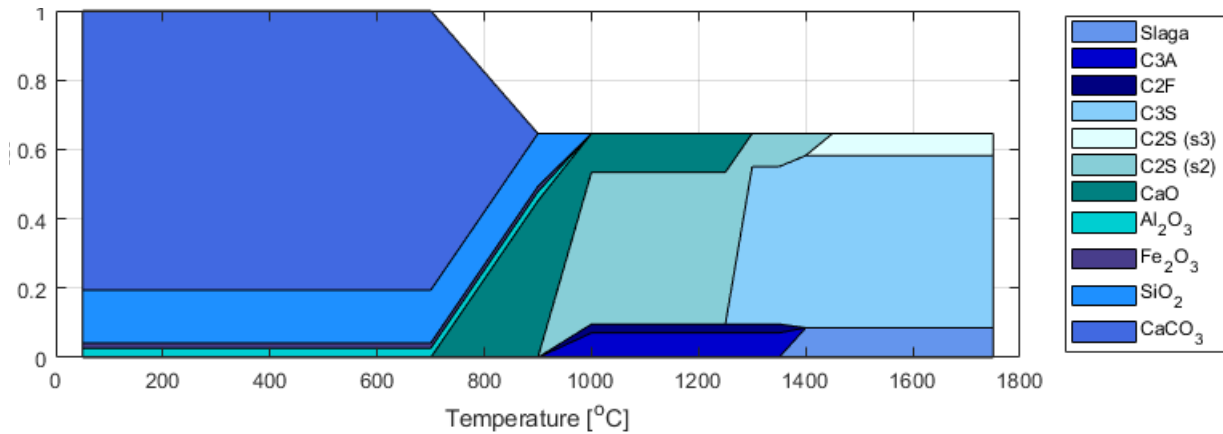


Figure 4.1: How the composition in a mass of 1 g changes through the temperature interval

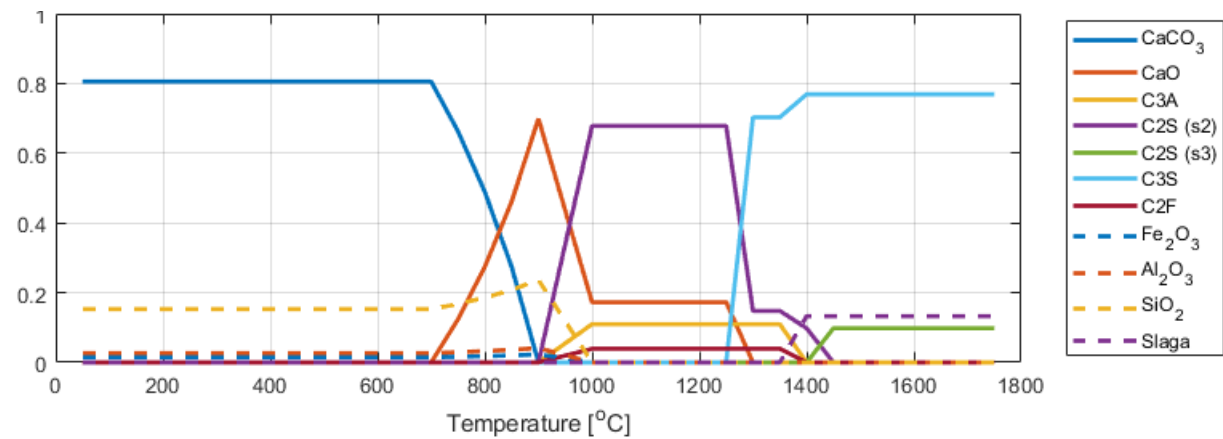


Figure 4.2: Mass fractions of the total mass of all species, depending on temperature

4.2 Energy Balances

Table 4.2 shows the total energy in percent compared to the current value at Slite, required to heat the meal from the inlet temperature of the cyclone tower, 87°C, to the outlet temperature of the kiln, which was 1394°C according to data from operational case 1 and 1451°C according to data from operational case 2. Also presented in the table is the total heat of reaction, and the change of heat content in the gas. The cyclone tower and kiln results are shown separately in Table 4.3. By comparing the sum of the energy need with the heat supplied through combustion, according to data from CEMENTA, an efficiency could be calculated for all parts. This efficiency describes how much of the fuel consumption provides useful heat, while the remaining heat is lost to the environment via radiation, conduction and air leakage. When the total change of heat content of the gas is negative, it is due to the enthalpy of gas entering the kiln being higher than the enthalpy of the gas exiting the cyclone tower, meaning energy has been released from the gas.

Table 4.2: Total energy need for heating the meal and for all reactions

Energy need [%]		
	Case 1	Case 2
Q_b	32.4	33.4
Q_{react}	52.0	53.4
Q_g	-17.7	-18.1
Sum	66.6	68.6
Q_{slite}	100	

Table 4.3: Energy need for heating the meal and for all reactions in the cyclone tower and rotary kiln

Energy need [%]				
	Cyclone Tower		Rotary kiln	
	Case 1	Case 2	Case 1	Case 2
Q_b	45.3	43.6	20.1	22.4
Q_{react}	94.6	83.5	12.7	21.3
Q_g	-42.9	-31.2	6.1	-4.1
Sum	96.0	95.9	38.9	39.6
Q_{slite}	100			

The efficiency of the heat transfer from combustion in the calciner was set to 95% which resulted in the temperature of gas exiting the kiln presented in Table 4.5. These temperatures are close to those presented in theory, leading to the chosen efficiency in the calciners appearing to be accurate. The calculated outlet gas temperature of the kiln was then used to calculate Q_{gas} in Table 4.3. When using that to recalculate the efficiency of the combustion in the calciners, the result was 96%. The calculated efficiency is close to the input efficiency, indicating that the result is robust.

Difficulties arose when trying to compare efficiencies over the pyrosystem and just the kiln from literature with the calculated values, due to all values found being over the entire production process. That meant that no values were found for the specific parts of the process that were calculated in this thesis. However, using the input data gathered from site in the heat flux model, an energy consumption similar to the one calculated, was received. A similar energy consumption means a similar efficiency of the rotary kiln, which indicates that the calculated efficiency over the kiln is credible.

Considering how the heat of formation varies along the rotary kiln, see Figure 4.3, there are four zones where reactions are present, and three zones where no reactions occur. First an endothermic zone where the uncalcinated material is calcinated. Second, an exothermic zone where free lime is consumed to form calcium silicates, followed by a zone without reactions. The fourth and sixth zones are both endothermic; forming C3S and SLAGA respectively. The energy consumed or generated in the zones are presented in Table 4.4. The length of the zones in the rotary kiln was set similarly to the temperature intervals and was not altered between heat flux runs due to it being to time consuming. More on dividing the reaction zones in Section 4.4.

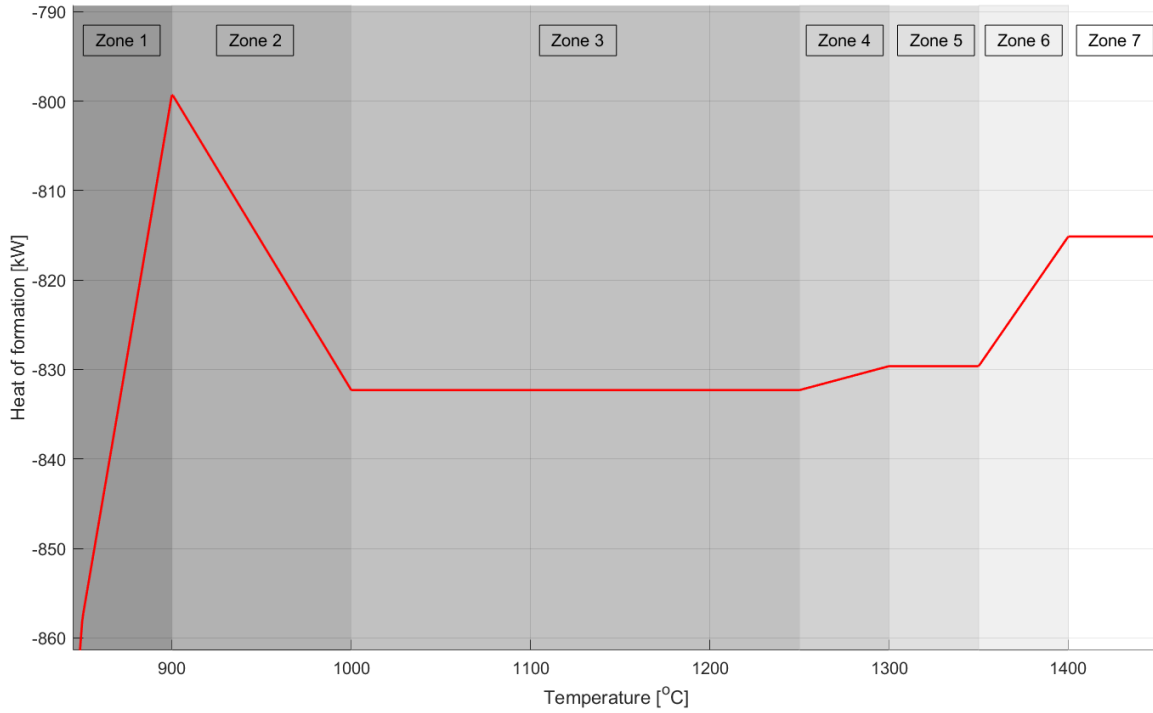


Figure 4.3: Graph of how the heat of formation varies along the temperature interval in the rotary kiln

Zone	Energy need [MW]	
	Case 1	Case 2
Q_{Z1}	32.1	40.7
Q_{Z2}	-31.7	-33.1
Q_{Z3}	0	0
Q_{Z4}	2.6	2.7
Q_{Z5}	0	0
Q_{Z6}	13.9	14.5
Q_{Z7}	-	0

Table 4.4: Reaction heat zones for the two operational cases in kiln in MW

The differences in reaction heat for the different operational cases are due to different product mass flows in the kiln. Zone 1 also differs due to a lower inlet temperature of the kiln in operational case 2 leading to more calcination occurring. The larger heat value of zone 6 is due to operational case 2 reaching a higher outlet temperature compared to operational case 1, and therefore completing the reactions and reaching a non-reaction zone. In real life there is probably more mass transfer occurring in the bed which should be taken into account and would alter the zones, possibly make them overlap. But as a radially well-mixed model over this system, the assumption of reaction zones is a good approximation.

4.3 Bed Modelling

From the energy balances solved in the model over the cyclone tower, meal temperatures were calculated as well as the temperature of the gas exiting the kiln. The resulting temperatures of the meal, seen in Table 4.5, are consistent with theory, with calcination initiating in the calciners and the meal being preheated in the cyclones. The reason for different temperatures in the north and south tower is the mass flow of meal not being divided equally between the north and south tower, and the gas temperatures in the towers differing.

Table 4.5: Calculated temperatures in the cyclone tower, case 1 and 2

Location	Temperature [°C]			
	Case 1		Case 2	
	North tower	South tower	North tower	South tower
Entering cyclone tower	87	87	87	87
After first double cyclone	405	404	409	392
After second cyclone	498	485	503	472
After third cyclone	520	526	536	530
After fourth cyclone	648	661	657	650
After calciner	845	847	854	851
After last cyclone	858	858	845	853
Gas exiting kiln	1050		881	

4.4 Heat Flux Model

Differing the lengths of the reaction zones did not change the results significantly. Lengths of 5, 15, 25, 10, 5, 15 and 5m was used for further modelling of both operational cases. The lengths of the zones were decided upon by consulting theory on the occurring reactions. Calcination being a highly spontaneous reaction at these temperatures, would lead to the material being calcinated in a short area in the beginning of the kiln. The rest of the zones were divided into similar lengths as the temperature steps.

Using the temperature vectors obtained from measurements of a rotary kiln in iron pelletisation industry and a flame temperature of 1800°C, a product temperature of only 1233°C can be reached. Therefore the flame temperatures received by Cementa were tested and the vectors were increased by different factors until desired product temperatures were reached.

Figure 4.4 shows results from the sensitivity analysis of contact factor, emissivity of wall and bed, and flame temperature, and how these parameters affect the heat transfer to the bed. The values are normalised to the resulting heat received by the bed when using the parameters shown in Table 3.1, to give a sense of how the changes would affect the total heat to the bed, measured in percent. The tested flame temperatures were based on numbers received from Cementa. Looking at the results of the sensitivity analysis, the emissivity of the wall does not impact the results much, which was expected. Increasing the emissivity of the bed leads to increased radiation from the meal particles, but also the absorption of energy due to the grey body assumption. Therefore, whether the amount of heat received increases or decreases depend on the temperatures of gas and bed used in Stefan-Boltzmann Law. The values for both emissivities set during the modelling were found in literature, which validated them. As the flame temperature increases the heat received by the meal increases significantly, therefore this is an important parameter that needs to be set accurately.

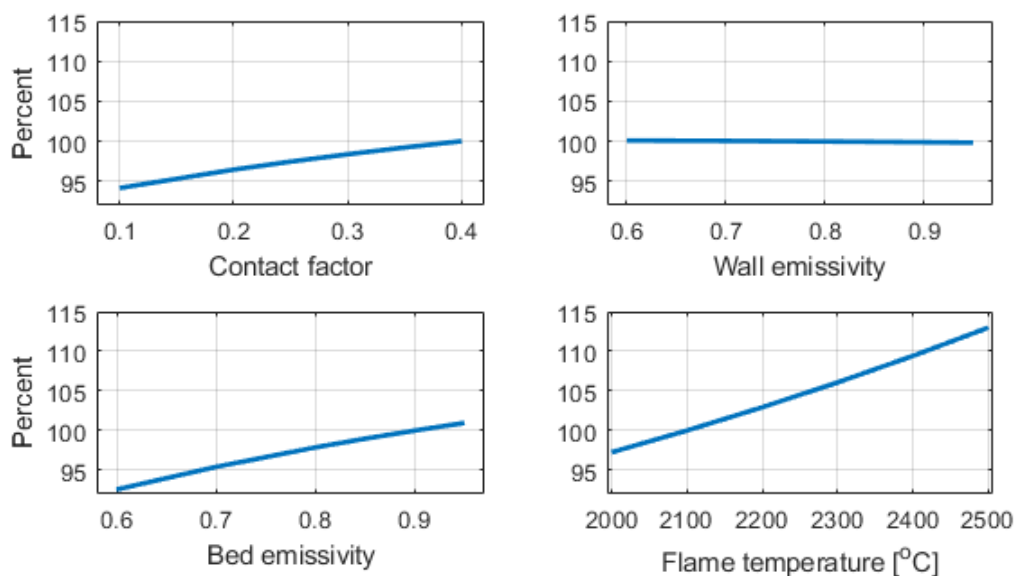


Figure 4.4: Graph of sensitivity analysis results normalised for heat received by bed

Different gas temperature profiles were tested to reach the correct product temperature and the ones shown in Figure 4.5 and 4.6 were used in further modelling in the coal cases due to it best describing the current operations at site and having the most reasonable appearance. The gas profiles obtained are used as input data to the model, which means that their appearance affects the result significantly. These profiles are unknown but a fair guess can be made considering temperature, length and radius of the flame, and gas outlet and inlet temperatures. Viewing the figures one can see the contours of the flame. The temperature vectors set to produce the gas profiles were increased by 6% for operational case 2 to reach the higher product temperature. Even though the energy consumption is lower in the second operational case, the mass flow of meal is larger, giving a larger volumetric flow of gas which can hold the heat longer, which results in a slower inclination of the profile.

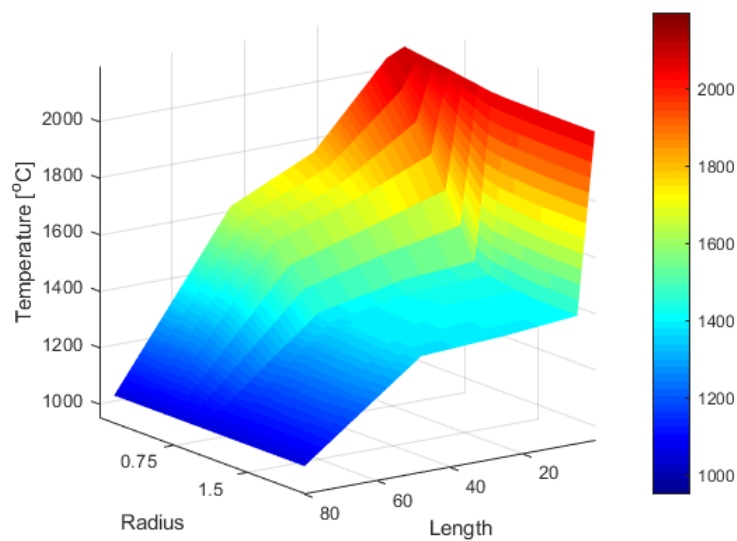


Figure 4.5: Graph of the gas temperature profile along the rotary kiln for case 1

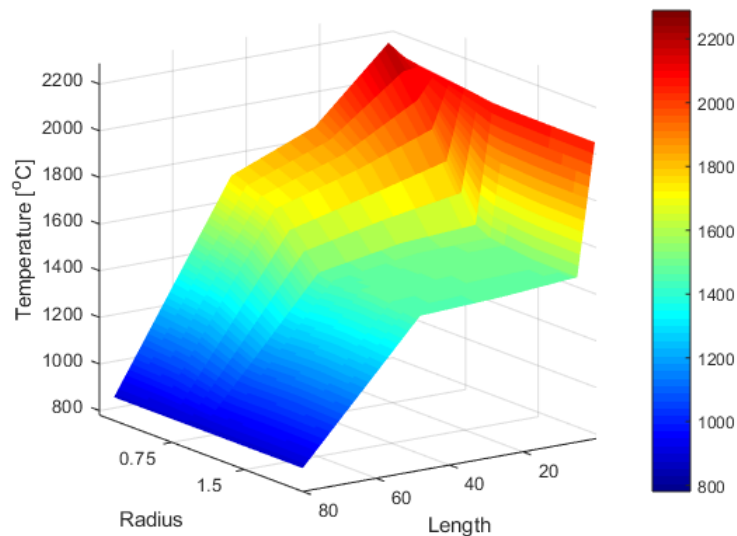


Figure 4.6: Graph of the gas temperature profile along the rotary kiln for case 2

Using mass fractions, heat capacities and heat of reaction added in the heat flux model, different contributions of the heat transfer mechanisms to the heat received by the meal in the rotary kiln can be observed. Figures 4.7 and 4.8 show heat fluxes of absorbed heat in the kiln for operational case 1 and 2. Comparing the fluxes between the two operational cases, they look very similar, except for an increase at about 50 m from the burner end, where the flux for operational case 2 is higher. This increase is due to a non-reaction zone (Z3), and the higher increase of the operational case 2 flux is due to higher radiation contribution compared to operational case 1, because of higher temperatures at that position and the larger volumetric gas flow. The fast decrease of the radiation contribution at the burner position in both operational cases is probably due to passing the flame to the less radiative nozzle of the burner where the temperature has not peaked yet. The contribution of convection from the gas is a small part of the total flux, which is reasonable compared to the other fluxes. Convection can only be transferred through the top layer of the meal bed while conduction transfers heat all around the bottom of the bed more effectively.

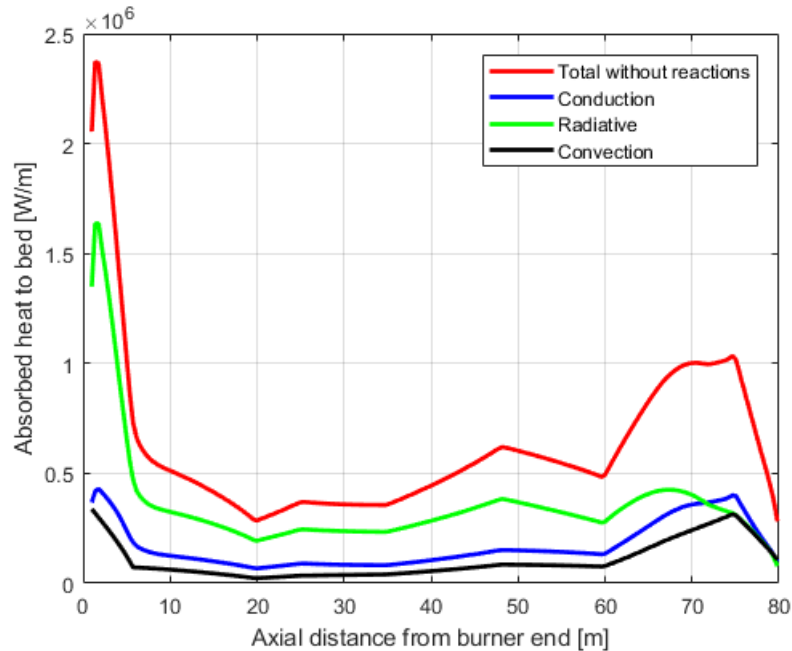


Figure 4.7: Graph of heat fluxes along the rotary kiln for case 1

Figures 4.9 and 4.10 show temperature profiles along the kiln for bed and wall plotted together with how the reaction heat varies through the kiln. They show a similar wall temperature profile along the kiln, which indicates that the gas profiles being different is acceptable. The wall temperature for operational case 1 does not get as cold during the first endothermic reaction zone as for operational case 2, again due to a larger endothermic contribution in operational 2. It also reaches 1500°C faster, due to the higher gas temperatures and increased radiative heat flux. The bed temperature profiles are also similar in shape but in operational case 2 does not go as low in temperature during the two endothermic reactions as in operational case 1. The lower temperature around 75 m from the burner end of the kiln is due to the first endothermic reaction being larger for operational case 2 than for operational case 1, as mentioned above.

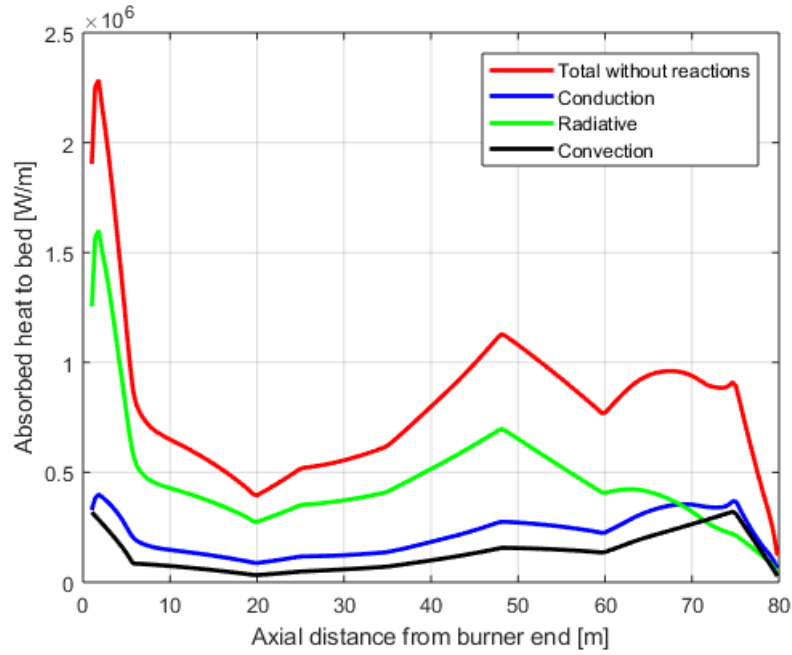


Figure 4.8: Graph of heat fluxes along the rotary kiln for case 2

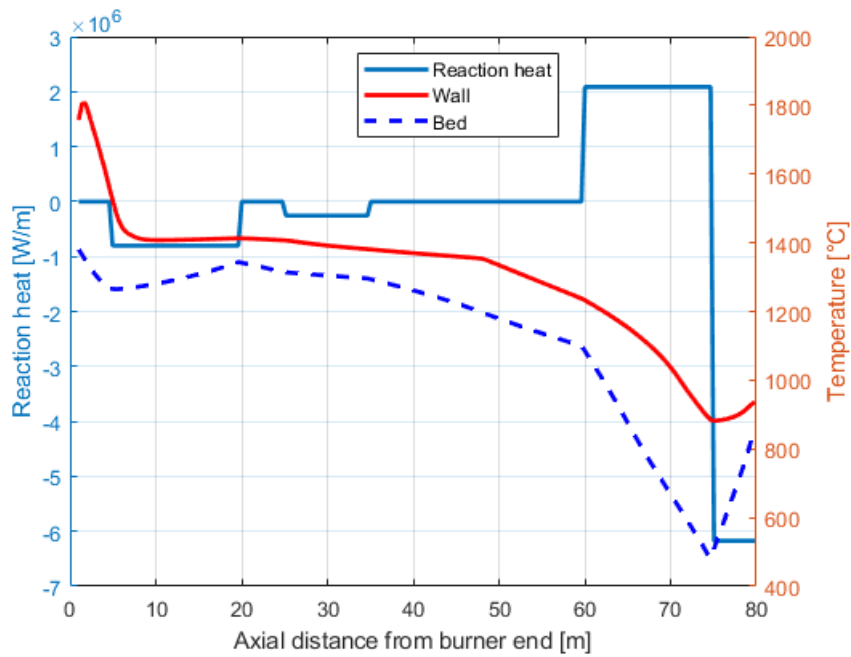


Figure 4.9: Graph of how the wall and bed temperatures and reaction heat vary along the rotary kiln for case 1

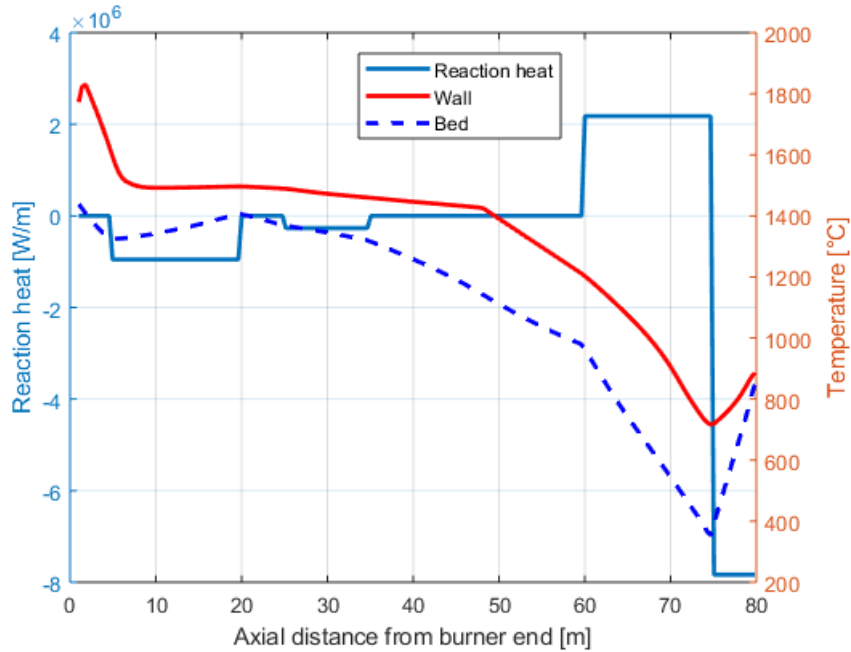


Figure 4.10: Graph of how the wall and bed temperatures and reaction heat vary along the rotary kiln for case 2

Table 4.6 presents the results of heat to the bed from the different heat transfers and the received outlet and product temperatures. The behaviour mentioned above is also visible when comparing the heat flux values in the table, with a larger heat of reactions for operational case 2 than for operational case 1. Also visible is that all fluxes are larger for operational case 2, probably due to the higher gas temperatures and larger volumetric gas flow. The resulting temperatures of the produced clinker from the heat flux model are close to what they should be according to operational data from Cementa, which validates that the model correctly simulates the current operation of the rotary kiln.

Table 4.6: Results from case 1 and 2 with coal burner

Parameter	Value		
	Case 1	Case 2	
Heat to bed total without reactions	34.3	38.9	MW
Heat to bed total with reactions	49.9	64.2	MW
Heat of Reactions	-15.2	-24.8	MW
Heat of Conduction	13.5	17.0	MW
Heat of Radiation	28.2	36.8	MW
Heat of Convection	8.2	10.4	MW
Sum	34.8	39.3	MW
Product temperature	1394	1451	°C

4.5 Plasma Modelling

Below follows the results extracted from the model for the plasma modelling, for which input data from operational case 1 was used. In Figure 4.11, the gas temperature profile used to achieve the results in Table 4.7 is shown. Figure 4.13 show the plotted heat fluxes and Figure 4.14 the reaction heat, and wall and bed temperature along the kiln. Based on the result of plasma modelling it appears to be a possible option to consider replacing the current burners with plasma torches. However, the results reached depend on the gas temperature profile used as input data. To validate these results, modelling or calculations would need to be performed on the gas temperature profile, to see if this profile can be achieved with the installed effect used. If not, a larger effect would need to be tested.

Figure 4.12 shows how the axial gas temperature profile in the plasma modelling case differs from the axial gas temperature profile used in the coal modelling, seen in Figure 4.6, with ΔT on the y-axis. The temperature difference is defined as $\Delta T = T_{gas,plasma} - T_{gas,coal}$.

Table 4.7: Results from plasma modelling

Parameter	Value
Heat to bed total without reactions	37.7 MW
Heat to bed total with reactions	54.3 MW
Heat of Reactions	-16.8 MW
Heat of Conduction	15.6 MW
Heat of Radiation	36.4 MW
Heat of Convection	2.4 MW
Sum	37.5 MW
Product temperature	1451 °C

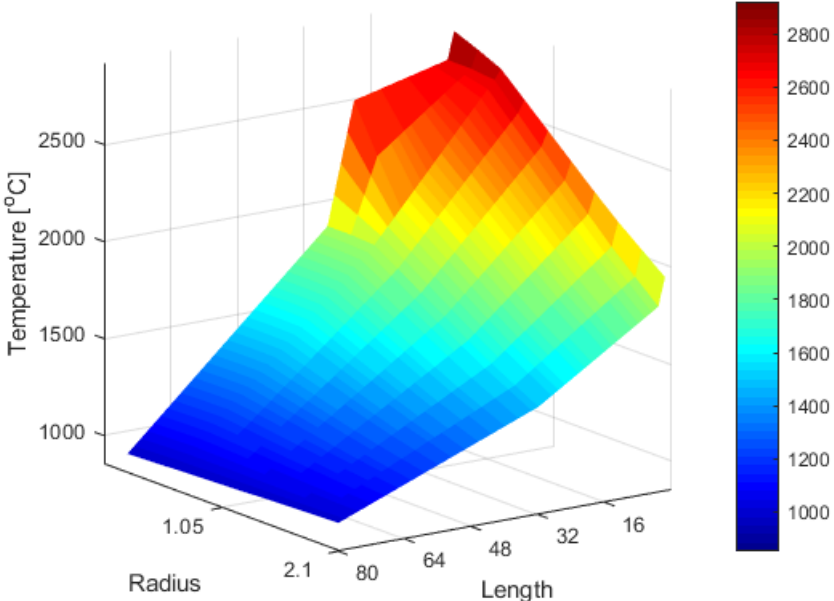


Figure 4.11: Graph of the gas temperature profile along the rotary kiln for plasma torch implementation

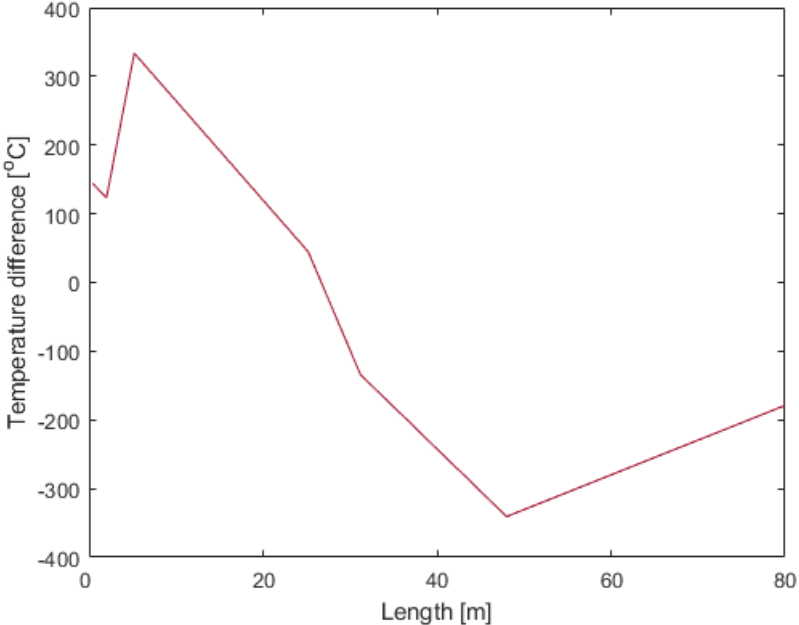


Figure 4.12: Graph showing the difference between the axial gas temperature profiles for the plasma modelling and for the coal modelling

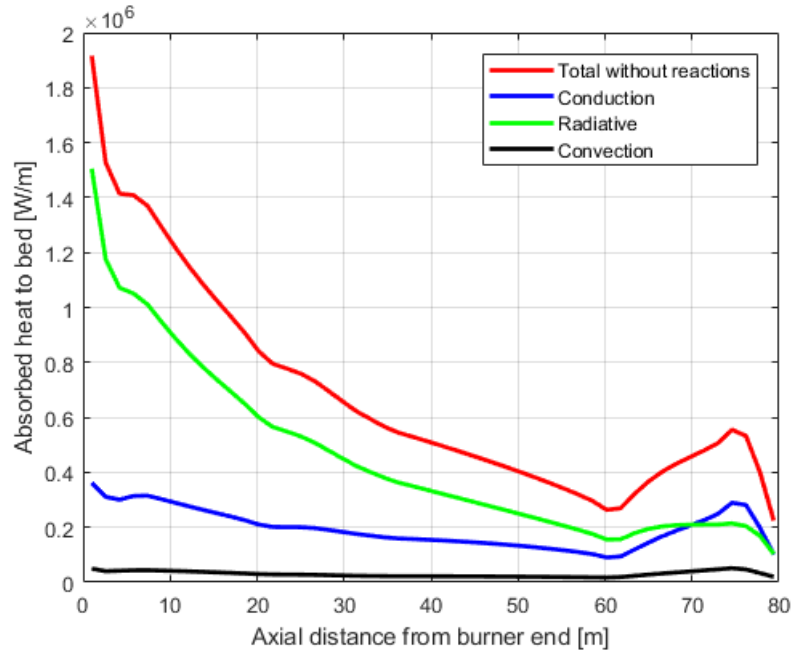


Figure 4.13: Graph of heat fluxes along the rotary kiln for plasma torch implementation

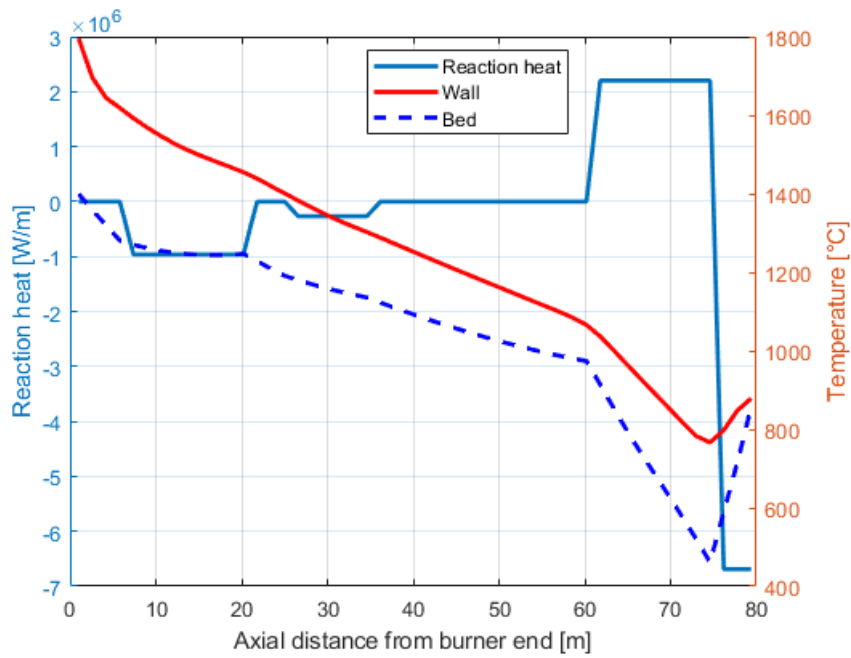


Figure 4.14: Graph of how the wall and bed temperatures and reaction heat vary along the rotary kiln for plasma torch implementation

5

Conclusion

The main result of this thesis is the developed heat transfer model of the rotary kiln and the approach for using it for modelling cement production.

The methodology used for modelling was deemed to be a good approach. Dividing the kiln into reaction zones and determining the reaction heat in a separate model, and then using it as input in the main model, ensured that the main model did not require too much computational time and still provided robust results. This is the approach recommended to be used for further modelling.

The heat transfer model was validated against the current production case, using a gas temperature profile which was created based on temperature data from Cementsa. The used gas temperature profile was deemed to be accurate, but a more correct estimate could be found by performing measurements in the current rotary kiln to re-validate the model. Another way to improve the accuracy of the gas temperature profile would be to include a combustion model to solve the gas temperatures, this is however a complex task, and was not deemed necessary. The validation was based on comparing the solved outlet temperature of the clinker with the outlet temperature according to process data. Based on this validation, the model could be used for evaluating the implementation of plasma torches.

The results of modelling plasma torches indicated that it is feasible to replace the fuel burners with plasma torches in the rotary kiln. To validate this result, calculations on the gas temperature profile in the kiln need to be performed to investigate if the required temperatures can be reached.

6

Suggestions for Further Research

The material data used in this model was assumed to be valid for cement production. However, there needs to be more research performed on the clinker reactions and their kinetics to make a more comprehensive model with time as a parameter. Since Cementa has planned to perform such research on cement chemistry, future plasma modelling could be performed with the results of this research.

As mentioned previously, the approach of using a separate model to calculate the reaction heat and concluding it in reaction zones was deemed to be valid. This approach could be improved by including the new cement chemistry, with reaction kinetics, and setting the length of each zone to corresponds with the rate of the reactions occurring in that zone, to have an accurate residence time of each zone. Corresponding the material temperature in the heat flux model with the temperatures of each reaction zone could be performed with an improvement like this. Another improvement would be to connect these two models, so that iterations between them would not need to be performed manually.

To improve the validity of the results from plasma modelling, the gas temperature profile used as input data needs to be correct. This could be achieved either by performing measurements with small scale plasma torches and scaling up the results, or by performing detailed modelling using Computational Fluid Dynamics (CFD) modelling of the gas phase temperature.

Bibliography

- [1] Bodil Wilhelmsson, Claes Kollberg, Johan Larsson, Jan Eriksson, and Magnus Eriksson. "Cemzero - A feasibility study evaluation ways to reach sustainable cement production via the use of electricity", Vattenfall and Cementa AB, 2018.
- [2] Jos G.J. Olivier, Greet Janssens-Mewnhout, Marilena Muntean, and Jeroen A.H.W. Peters. "Trends in global CO₂ emissions: 2016 report", PBL Netherlands Environmental Assessment Agency, Hague, Netherlands, 2315, 2016. [Online]. Available: <https://www.pbl.nl/sites/default/files/cms/publicaties/pbl-2016-trends-in-global-co2-emissions-2016-report-2315.pdf>, Accessed on: Jan 21, 2019.
- [3] Verein Deutscher Zementwerke. "Global cement production from 1990 to 2030 (in million metric tons)". [Online]. Available: <https://www.statista.com/statistics/373845/global-cement-production-forecast/>, Accessed on: Jan 21, 2019.
- [4] Jocelyn Timperley. "Q&A: Why cement emissions matter for climate change". *CarbonBrief: clear on climate*. Sep. 2018. [Online]. Available: <https://www.carbonbrief.org/qa-why-cement-emissions-matter-for-climate-change>, Accessed on: Jan 27, 2019.
- [5] Anders R.Nielsen. "Combustion of large solid fuels in cement rotary kilns", Ph.D. dissertation, Department of Chemical and Biochemical Engineering, Technical University of Denmark, Lyngby, Denmark, 2012. [Online]. Available: [http://orbit.dtu.dk/en/publications/combustion-of-large-solid-fuels-in-cement-rotary-kilns\(0643a7be-05bb-4625-afc1-6e6314de5632\).html](http://orbit.dtu.dk/en/publications/combustion-of-large-solid-fuels-in-cement-rotary-kilns(0643a7be-05bb-4625-afc1-6e6314de5632).html), Accessed on: Jan 25, 2019. 2012.
- [6] Karin Byman. "Reliability in Sweden's electricity system: A project report", The Royal Swedish Academy of Engineering Sciences, Stockholm, Sweden, 489, 2017. [Online]. Available: <https://www.iva.se/globalassets/info-trycksaker/vagval-el/201705-iva-vagvalel-leveranssakerhet-english-c.pdf>, Accessed on: Feb 18, 2019.
- [7] Åke Truedsson. "Cementprocessen, från kalksten till färdig cement", Unpublished. Cementa AB.
- [8] Bodil Hökfors. "Phase chemistry in process models for cement clinker and lime production", Ph.D. dissertation, Department of Applied Physics and Electronics, Umeå Universitet, Umeå, Sweden, [2014]. Available: <https://www.diva-portal.org/smash/get/diva2:696534/FULLTEXT01.pdf>, Accessed on: Jan 21, 2019.

- [9] Bodil Wilhelmsson, Johan Larsson, and Project leaders at Cementa Stefan Sandelin. Private communication, February 2019. Project Leaders at Cementa.
- [10] Robert J. Goldston and Paul H. Rutherford. "Introduction to plasmas" in. *Introduction to Plasma Physics*. Bristol, United Kingdom: Institute of Physics Publishing, 1995, ch. 1, pp. 1-2. [Online]. Available: http://www.astrosen.unam.mx/aceves/verano/libros/goldstone_plasma.pdf, Accessed on: Feb 12, 2019.
- [11] Patrick P Taylor and Shahid A Pirzada. "Thermal plasma processing of materials: A review", *Advanced Performance Materials*, vol. 1, no. 1, pp. 35-50, Jan. 1994. doi:10.1007/BF00705312 [Online]. Available on: ResearchGate, <https://www.researchgate.net/>, Accessed on: Feb 12, 2019.
- [12] S.L. Camacho. "Industrial-worthy plasma torches: State-of-the-art. *Pure and Applied Chemistry*. vol. 60, no. 5, pp. 619-632, 1977. doi:10.1351/pac198860050619. [Online]. Available: ResearchGate, <https://www.researchgate.net/>, Accessed on: Feb 12, 2019.
- [13] N. Venkatramani. "Industrial plasma torches and applications", *Current Science*, vol. 83, no. 3, pp. 254-262, Aug. 2002. [Online]. Available on: JSTOR, <https://www.jstor.org/>, Accessed on: Feb 11, 2019.
- [14] M.F. Zhukov, I.M. Zasytkin, A.N Timoshevskii, B.I. Mikhailov, "Brief description of thermal plasma G.A. Desyatkov, and electric heating of gas" in. *Thermal Plasma Torches: Design, Characteristics, Applications*. M.F. Zhukov and I.M. Zasytkin. Cambridge, Great Britain: Cambridge International Science Publishing, 2007, ch. 1, pp. 8-13. [Online]. Available: <http://www.itam.nsc.ru/upload/medialibrary/76c/plasma-heaters.pdf> , Accessed on: Feb 15, 2019.
- [15] Alexandra von Meier. "The Physics of Electricity" in. *Electric Power Systems: A Conceptual Introduction*. Hoboken, United States of America: John Wiley & Sons. Inc, 2006, ch. 1, pp. 14-15. [Online]. Available: <http://personal.psu.edu/sab51/vls/vonmeier.pdf>, Accessed on: Feb 15, 2019.
- [16] Daniel Sundberg Energy Engineer at ScanArc. Private communication, May 2019.
- [17] Lakshminarayana Rao, Pierre Carabin, and F. Rivard. "Thermal plasma torches for metallurgical applications". *TMS Annual Meeting*. pp. 57-65, Feb. 2013. doi10.1002/9781118663448.ch8, [Online]. Available: ResearchGate, <https://www.researchgate.net/>, Accessed on: Feb 11, 2019.
- [18] P.V. Ananthapadmanabhan and N. Venkatramani. "Chapter 6 Thermal plasma processing". *Pergamon Materials series*. vol. 2, pp. 121-150, 1999. doi:[https://doi.org/10.1016/S1470-1804\(99\)80052-2](https://doi.org/10.1016/S1470-1804(99)80052-2). [Online]. Available: ScienceDirect, <https://www.sciencedirect.com/>, Accessed on: Feb 11, 2019.
- [19] R. Stuart Haszeldine. "Carbon Capture and storage: How Green Can Black Be?", *Science*, vol. 325, no. 5948, pp. 1647-1652, Sep. 2009. [Online]. Available: <https://science.sciencemag.org/content/325/5948/1647>, Accessed on: Mar 8, 2019.
- [20] M. E. Boot-Handford, J. C. Abanades, E. J. Anthony, M. J. Blunt, S. Brandani, N. Mac Dowell, J. R. Fernandez, M.-C. Ferrari, R. Gross, J. P. Hallett, R. S. Haszeldine, P. Heptonstall, A. Lyngfelt, Z. Makuch, E. Mangano, R. T. J. Porter,

- M. Pourkashanian, G. T. Rochelle, N. Shah, J. G. Yoo, and P. S. Fennell. "Carbon Capture and storage update", *Energy & Environmental Science*, vol. 7, no. 1, pp. 130-189, July 2014. doi:10.1039/C3EE42350F, [Online]. Available: Royal Society of Chemistry, <https://pubs.rsc.org/>, Accessed on: Mar 8, 2019.
- [21] Jon Gibbins and Hannah Chalmers. "Carbon Capture and storage", *Energy Policy*, vol. 36, no. 12, pp. 4317-4322, Dec. 2008. doi:10.1016/j.enpol.2008.09.058, [Online]. Available: ScienceDirect, <https://www.sciencedirect.com/>, Accessed on: Mar 8, 2019.
- [22] Stephen A. Rackley. "Carbon capture technologies" in. *Carbon Capture and Storage*. Amsterdam, Netherlands: Elsevier Inc, 2017, ch. 1, pp. 5-16. [Online]. Available: <https://www.sciencedirect.com/book/9780128120415/carbon-capture-and-storage>, Accessed on: Mar 8, 2019.
- [23] Anders Lyngfelt Professor at Chalmers University of Technology. Private communication, May 2019.
- [24] Howard Herzog and Dan Golomb. "Carbon capture and storage from fossil fuel use". *Encyclopedia of Energy*. vol. 1, pp. 277-287, Dec. 2004. doi:10.1016/B0-12-176480-X/00422-8, [Online]. Available: ResearchGate, <https://www.researchgate.net/>, Accessed on: Mar 5, 2019.
- [25] Mann and Kump. *Dire Predictions: Understanding Climate Change*. Pearson Education, Inc, 2015. London, England: Pearson Education, Inc. 2015. Print.
- [26] Chinmay Ghoroi and A. K. Suresh. "Solid–solid reaction kinetics: Formation of tricalcium aluminate" *ALChE Journal*, vol. 53, no. 2, pp. 502-513, Feb. 2007. doi: 10.1002/aic.11086, [Online]. Available: ResearchGate, <https://www.researchgate.net/>, Accessed on: May 1, 2019.
- [27] Adrian Gunnarsson, Klas Andersson, and Bradley Adams. "Full Scale 3D-modelling of the Radiative Heat Transfer in Rotary Kilns with a Present Bed Material" in *Clearwater Clean Energy Conference*, 2018.
- [28] J.P. Gorog, T.N. Adams, and J.K. Brimacombe. "Regenerative Heat Transfer in Rotary Kilns", *Metallurgical and Materials Transactions B*, vol. 13, no. 2, pp. 153-163, June 1982.

